Estimation of the 'Investible Space' in Macro Investment Environments for Clean Energy Investments

Sumit Kothari*, Nadia Ameli
University College London

14 February 2025

Abstract

Investments in mainstream renewable energy technologies are increasingly driven by a preferential financial risk assessment against a market-rate return across public and private actors. A variety of macro risks characterise a complex investment environment defining its suitability for clean energy investment. Using machine learning models, this study aggregates the risk environments of funded solar energy projects to construct an 'investible space' i.e. the set of environments perceived to be most suitable for investments by financial markets. It identifies the frontiers of this space in terms of the relative acceptability of different risks and identifies opportunities to mitigate risks by understanding their patterns of co-occurrence. Risks balance, accentuate, correlate and combine in distinct ways to produce non-linearity in investment outcomes such that investors react to combined risk configurations. Understanding macro risk interactions provides opportunities to design de-risking strategies that are efficient and effective in different economic and governance environments across countries. Such strategies can foster a broader, more equitable distribution of climate finance, ensuring that diverse investment environments become viable for mitigation projects.

* Contact: sumit.kothari@ucl.ac.uk

Introduction

The rapid fall in the cost of renewable energy technologies, particularly solar photovoltaics and wind energy, over the last two decades has made them competitive with fossil-fuel based electricity generation in countries around the world (IRENA, 2024). This trend has emerged despite the variation in project costs across countries that are influenced by local economic environments, technical capacities and institutional settings, alongside the natural variation in solar and wind resources. Energy system models increasingly show that renewable energy technologies, particularly solar energy, will come to dominate the energy mix of countries as their costs continue to decline, thereby making them the cheapest source of energy worldwide (Nijsse *et al.*, 2023; IEA, 2024). Decades of declining life-time energy costs for mainstream renewable energy technologies has however not translated to their widespread deployment across different regions. This is despite the commoditization and mass production of components, such as solar panels, the political tailwinds for decarbonisation, strong international push towards renewable energy deployment and the positive socio-economic impacts of affordable, sustainable energy.

The future expansion of renewable energy within global energy systems is significantly constrained by the limited availability of adequate finance for potential projects across countries. This challenge is especially acute for many middle- (MI) and low-income (LI) countries[1] for whom solar energy is the most accessible and scalable renewable energy technology, but which struggle to raise sufficient low-cost capital for solar projects (Donastorg, Renukappa and Suresh, 2017). Unlike high-income (HI) countries, where private finance provides the majority of investments for commercially viable renewable energy projects (Songwe, Stern and Bhattacharya, 2022), low capital stock and underdeveloped financial markets in MI and LI countries constrain their potential for raising private finance locally (Ameli *et al.*, 2021). Public finance, mobilised domestically and through bilateral and multi-lateral channels, has reached financing limits due to constrained capacities, competing national priorities and weak international commitment. International private finance markets have therefore increasingly been called upon to bridge the funding gap for large-scale renewables rollout in MI and LI countries, often

[1] According to the income-based classification of countries developed by the World Bank. Available at: https://datahelpdesk.worldbank.org/knowledgebase/articles/906519-world-bank-country-and-lending-groups

mobilised using public finance investments through blended finance structures (Bhattacharya *et al.*, 2024).

Much of the financing by public and private actors to renewable energy projects is currently delivered at 'market-rate' and depends on the financial market's assessment of risks associated with these projects (CPI, 2023b). Given that these investments are largely made up-front, at the time of project development, any future fluctuation in project conditions can directly impact the returns that investors expect over their long lifespan (Steffen, 2020). These relate to changes in important parameters relating to a project's development, construction and continued operation that affect the development costs, gestation period and future revenues of the project (Raikar and Adamson, 2020). Projects that are perceived as inherently risky thus often face high costs of capital, and beyond certain thresholds of risk, these may simply become uninvestible.

Broadly, the risks associated with renewable energy projects may be classified into technological risks, macro risks and project-specific risks. Technology risks relate to fundamental uncertainties typically associated with a technology such as uncertainties in performance, output, failure rates, longevity, design stability and learning potential that affect all projects irrespective of their geography. These are quite characteristic of nascent technologies that have yet to be proven with deployment across regions and climactic conditions at scale. Macro risks cover the attributes of the individual country context in which the project is deployed and span the macroeconomic, industrial and policy environment in which a project is developed and functions, such as political, currency and credit risks. Finally, project-specific risks concern the risks that are idiosyncratic to specific projects beyond the general country context and may include a range of factors such as geographic challenges, site-specific technological configurations, supply-chain costs, local permit issues, availability of skilled technicians, construction risks and environmental risks.

As mainstream renewable energy technologies have been widely deployed across different regions and climactic conditions, their performance and reliability have become well understood and therefore technological risks are considered relatively easy to manage (Egli, 2020). Similarly, project-specific risks tend to decline with increasing project development experience in a country (Persaud, 2023), likely due to sectoral learning-by-

doing processes that enhance project management capabilities and better align regulatory processes. These are fundamentally considered to be business risks that developers bear as part of their business operations to earn profits. Additionally, it is also possible to transfer many of these risks to insurance companies, government agencies or other public entities such as development banks. Macro risks however stem from the broader investment environment, comprising economic, political and governance factors in a country as well as the specific market and policy landscape for renewable energy. These risks are difficult to transfer, diversify or mitigate completely, while substantially impacting project outcomes (IRENA, 2016).

A variety of macro risks characterise a complex investment environment and define its suitability for investment based on the perception of diverse investors in financial markets – irrespective of the technological suitability and market viability of mainstream renewables. Many studies have highlighted the range of factors that may affect the perception of the investment environment and create barriers that lead to limited availability of capital, high capital costs (leading to high energy prices) and chronic underdevelopment of the renewable energy industry (Hu *et al.*, 2018; Ouedraogo, 2019; Emodi *et al.*, 2022). Conducive investment environments will attract domestic and foreign capital at lower costs and at a greater scale, particularly in MI and LI countries. For instance, Persaud (2023) and CPI (2023a) use stylised calculations to show the substantial impact that foreign exchange and credit risks have on the cost of capital for renewable energy projects in these countries and the improvements that mechanisms to reduce these risks can potentially achieve. Mitigating critical risks in the investment environment is thus essential to induce private and public capital across countries and needs a greater consideration in the design of an international climate finance architecture.

A quantitative characterisation of the investment environment in terms of its major component risks can identify the independent and joint effect that these have on making a country conducive for investment. Using machine learning models, this study aggregates the risk environments corresponding to funded solar energy projects to construct an ‘investible space’ i.e. the set of environments perceived to be most suitable for investments by financial actors. It describes conducive investment environments in terms of the relative acceptability of different risks and identifies opportunities to mitigate

risks by understanding their patterns of co-occurrence. In doing so, it captures the non-linearities of the changes in investibility with changes in the level of individual risk factors and the potential tipping points that are triggered due to combined impacts of changes across multiple risk factors. It thus provides a macro complement to existing micro studies that use simulation techniques to evaluate the uncertainty in economic and policy variables on stylised plant-level cashflows (Fuss *et al.*, 2008; Pereira *et al.*, 2014; Afanasyeva *et al.*, 2016).

Methods

Macro Risk Indicators

This study evaluates eight macro-meso risk factors that have been identified in numerous studies to play an important role in investment decision-making for renewables (Waissbein *et al.*, 2013; Ioannou, Angus and Brennan, 2017; Egli, 2020). These are briefly described in Table 1 with further details provided in Appendix A.

Risk Factor	Description	Indicator
Foreign Exchange Risk	Risk associated with the variability in exchange rates of the domestic currency in which the project revenues are earned against foreign currencies in which investments are made	Annualised value of the standard deviation across a 5-year moving window of the log returns of monthly exchange rates of domestic currencies against the International Monetary Fund's Special Drawing Rights
Interest Rate Risk	Risk originating from the variability in the benchmark short-term interest rates against which loans are typically benchmarked	Annualised value of the standard deviation across a 2-year moving window of monthly changes in annual interest rates
Growth Risk	Risks emanating from cyclical movements in the broader economy of a country where the project is located	Average quarter-on-quarter real GDP growth rate in domestic currency of the previous 4 quarters
Sovereign Risk	Risks associated with the creditworthiness of the country's government where a project is located	A debt service coverage ratio defined as the gross debt position of the government divided by government revenue, which is downscaled by the GDP per capita indicating the revenue raising capacity of the government
Offtaker Credit Risk	Risks associated with the creditworthiness of the counterparty or the offtaker to whom the power from the project is contractually supplied	The Counterparty Risk score from the RISE indicators produced by the Energy Sector Management Assistance Program and the World Bank

Political Risk	Risks emanating from the stability of the political system in the country where the project is located	The Political Stability and Absence of Violence/Terrorism indicator from Worldwide Governance Indicators compiled by the World Bank
Institutional Risk	Risks created due to shortcomings in the governance, legal and regulatory environment of the project country	Aggregate of four indicators from the Worldwide Governance Indicators compiled by the World Bank: Government Effectiveness, Regulatory Quality, Rule of Law and Control of Corruption
Renewable Energy Policy Risks	Risks originating from the deficiencies and uncertainties in the policy environment for the renewable energy sector	Aggregate Renewable Energy indicator from the RISE indicators produced by the Energy Sector Management Assistance Program and the World Bank

Table 1: Description of risk factors and indicators

The data for the eight indicators representing individual risk factors is assembled for the set of 92 countries in consideration covering the 2010 – 2018 period. This dataset characterises the investment environment in each country at different points in time. In addition, the study uses investment data from the Bloomberg New Energy Finance database (BNEF, 2023) that covers over 26,000 investment transactions made in solar projects across the 92 countries from 2010 – 2018. This data provides the location and timing of investments for renewable projects and based on this a corresponding risk environment is characterised for each project using the risk factor indicators. The risk data is transformed and normalised for ease of interpretation and outliers that are beyond the 99^{th} percentile are removed.

The n-Dimensional Hypervolume

The macro investment environment can be characterised as a geometric space with the component risk factors as its dimensions or axes. These axes define a n-dimensional Euclidean space within which a geometric shape can identify the combination of risk factor values that constitute a conducive investment environment for renewable energy projects – *the investible space*. The features of this geometric shape, referred to as a hypervolume, provide information about the investible environment through its frontiers, surface and volume (Blonder *et al.*, 2014). Delineating a continuous n-dimensional hypervolume using discrete points of successful investments involves making assumptions about the neighbourhood of the observed data points since there is no information on where investments can't occur. The delineation process, in general, involves identifying a hypervolume function based on input data points that converts an n-dimensional vector of

risk values along the independent axes into a scalar probability of occurrence or a binary presence/absence indicator at any point in the hyperspace. The hypervolume function then needs to be applied to an appropriate region of the hyperspace to delineate the boundaries of the hypervolume. This process needs to sample a large number of random points in high dimensional space to accurately identify the boundaries of the hypervolume (Blonder *et al.*, 2014).

This study employs two machine learning algorithms to discern the hypervolume function: one-sided support vector machines (SVM) and gaussian kernel density estimation (KDE), as described in detail in Blonder et al. (2018) and summarised below.

One-Class Support Vector Machine (SVM)

SVMs are high-performance supervised learning algorithms that are widely used for classification problems with labelled data (Hearst *et al.*, 1998). These algorithms separate data into *n* different classes by finding the optimal *(n-1)* dimension hyperplane between data points that achieve a high degree of separation between them. Non-linear separation planes and loss functions are typically employed in difficult classification problems, usually found in real-world data, to achieve a high degree of classification while also maintaining a large margin of separation across classes. This hyperplane serves as a decision function, which once learned from existing data can be used to classify new data points into different groups.

SVMs have also been extended to a one-class case where the algorithm learns a decision function that defines a class boundary using observed data and can classify a new data point as similar or outlier compared to the observed set (Schölkopf *et al.*, 1999). Such a one-class SVM algorithm is used in this study to delineate hypervolumes. It learns a hypervolume function from presence-only input data i.e. the risk environments where investments have occurred, to identify regions of hyperspace that should be included in the hypervolume by making binary inclusion/exclusion predictions on sampled data points.

Gaussian Kernel Density Estimation (KDE)

KDE is a non-parametric method to estimate the probability density function of a random variable from a finite data sample by using a kernel function to weigh data points (Hastie, Tibshirani and Friedman, 2008). It learns the functional form of the distribution from input

data without making any assumptions about the underlying population distribution. KDE can be considered as “a sum of bumps” located at the observed data points with the shape of the bump determined by a chosen kernel function with a specified width i.e. the kernel function represents a probability distribution function centered at observed data points. For a symmetrical kernel function, the exact shape of the function has been found to have little effect on the estimation of the overall probability density function itself (Silverman, 2018). However, a Gaussian kernel function is advantageous as it provides a smooth output and is computationally fast (Węglarczyk, 2018).

For estimating the hypervolume function, a Gaussian kernel function is used to generate a padded region around an input data point. This region represents the potential set of points that may be included in the hypervolume with a probability defined by the Gaussian kernel function. The hypervolume function is then defined as a mixture density of individual Gaussian kernel functions (McLachlan, Lee and Rathnayake, 2019) i.e. the kernel functions centered at each observed data point are aggregated and normalised across data points to yield a hypervolume function. This hypervolume function assigns values to sample points based on their geometric proximity to input data points so that points closest to the input data points have the highest values and the function value decays asymptotically to zero for the farthest points.

A Monte Carlo approach is used to generate random data points using a hyperelliptical sampling algorithm. This algorithm takes a probabilistic approach and generates random points within a certain distance of the observed points that have a high probability of being included in the hypervolume. The points enclosed by Hyperellipses are multi-variate Normal and thus setting a fixed radius of the hyperellipse around a data point ensures that the sampled points represent all regions of hyperspace with a function value above an equivalent probability threshold. This approach seeks to strike a reasonable balance between sampling enough regions of the hyperspace and the computational cost of evaluating irrelevant data points. Using this approach, a uniformly random set of points are generated across the entire hyperspace, which are then evaluated using the hypervolume functions generated using the two algorithms to delineate the hypervolume shape. Further details about hypervolume estimation and a sensitivity analysis of tuning parameters is provided in Appendix B and Appendix C.

The two methods of hypervolume estimation take different approaches to delineating hypervolumes: KDE provides a continuous probabilistic output and therefore assigns a probability to all points of the generated random sample. The hypervolume is then delineated based on a selected probability threshold and provides a loose wrap around the input data. SVM in contrast provides a tighter fit around the data and creates a boundary that classifies points as within or outside the hypervolume. Consequently, the two methods of defining hypervolumes are used to analyse different aspects of the investment environment: a probabilistic approach is used to measure the suitability level of investment environments whereas the inclusion/exclusion method is used to understand the suitable range for individual risk factors in conducive environments and the complex shapes formed through their interaction.

The study uses the *hypervolume* package in R (Blonder, 2023) for hypervolume estimation using the KDE and SVM methods and for further analysis of hypervolume features.

Results

The Investible Space

Investment decisions for renewable energy projects are a function of a project's macro risk environment. The successful financing of a project constitutes an acceptance of the level of macro risk facing investors and therefore a funded project's risk profile can be considered suitable for investment. The hypervolume thus represents an investible space for renewable energy project since it aggregates risk profiles across many funded projects. The geometric representation of this investible space in the form of a tightly-fitted hypervolume created using the SVM model is shown in Figure 1. This figure shows 2-dimensional plots as combinations of the risk factors that represent the 8 dimensions of the hypervolume. It indicates the complex and non-linear response of investments to different levels of individual risks and the combinations of different risks found across the 92 countries over the time period of the study. The contour line in each of the plots shows the investment frontier in terms of the modelled macro risks. Projects beyond this frontier fall outside the investible space and will have a low probability of receiving investment, based on past investment decisions. The area of the enclosed space within the contour (and the volume of the 8-dimensional hypervolume) indicates the range of risk space that is considered favourable by investors. A narrow area indicates a smaller range of risk levels that are considered favourable and vice versa.

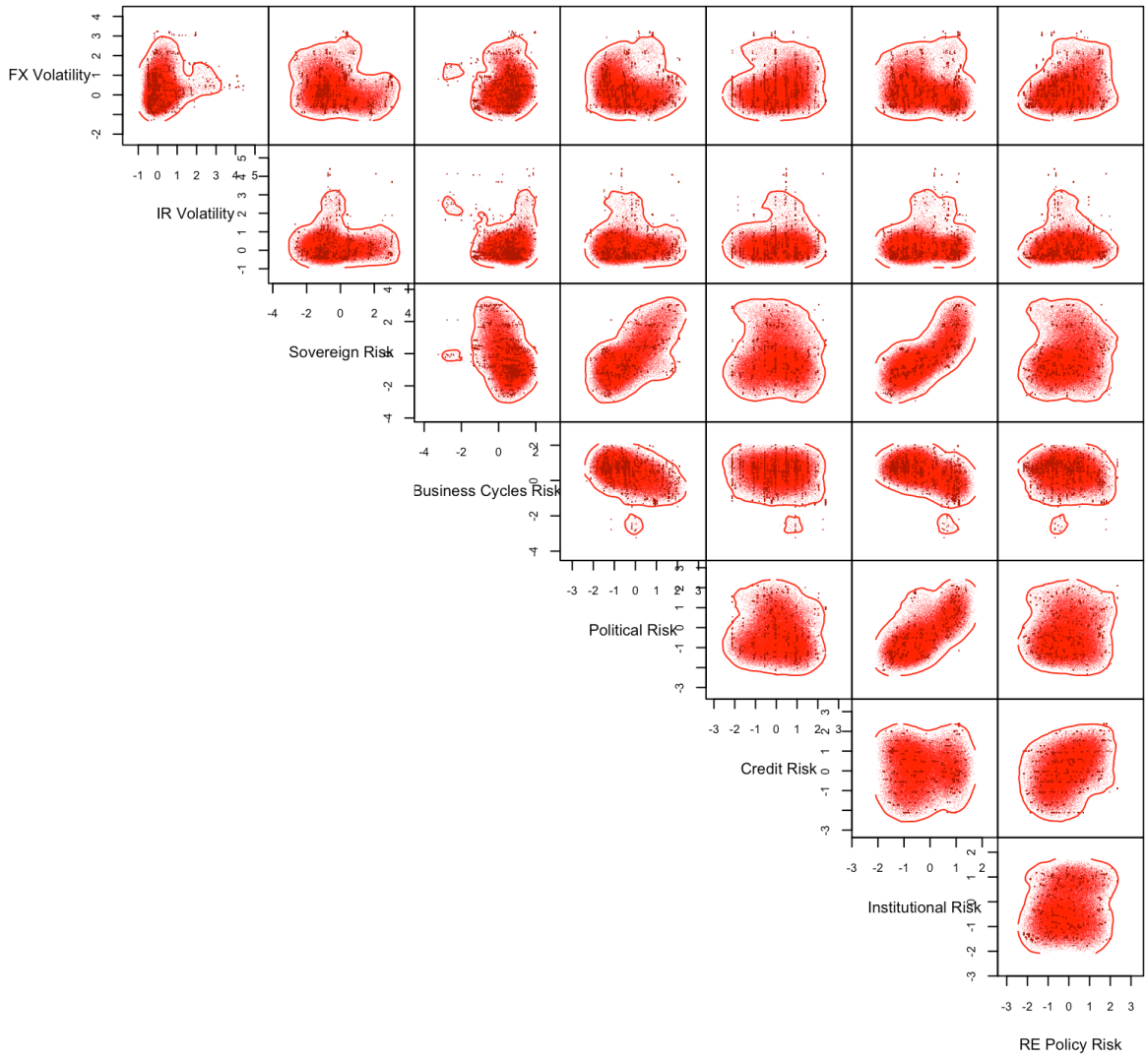


Figure 1: Hypervolume estimation using Support Vector Machine (SVM) algorithm with 200 random points per data point. 2-dimensional plots of all 8 axes dimensions. Axes indicate the range of variable values in standard deviations.

Distribution of Risk Levels in the Investible Space

Different levels of individual risks create non-linear outcomes for investment suitability. Examining the distribution of different macro risks within the investible space provides insight into their relative acceptability to investors (Figure 2). This analysis goes beyond a simple understanding of the risk envelope i.e. a range of acceptable values, by indicating the relative probability of different levels of risk to be considered suitable for investments. Foreign exchange risks, interest rate risks and growth risks are concentrated in the higher risk space (positive values) but display a relatively narrow range of highly suitable values (stronger colours). This indicates that while moderately high values for these risks are generally acceptable, they need to be confined within a fairly narrow range. Suitable levels of foreign exchange and interest rate risks however extend out towards a high maximum,

implying that in certain conditions, higher level of these risks may be acceptable, but with a low probability. Sovereign, political and institutional risks, on the other hand, are centered prominently in the lower risk space, implying that suitable investment environments typically exhibit low levels of these risks. Acceptable levels of sovereign and political risks are spread across a wide range with a greater tolerance for higher risk values, reflecting the environments in some MI and LI countries that receive investments to some degree despite high levels of these risks. Growth and institutional risks, meanwhile, have low upper limits indicating limited investor tolerance for low-growth economies and weak governance contexts.

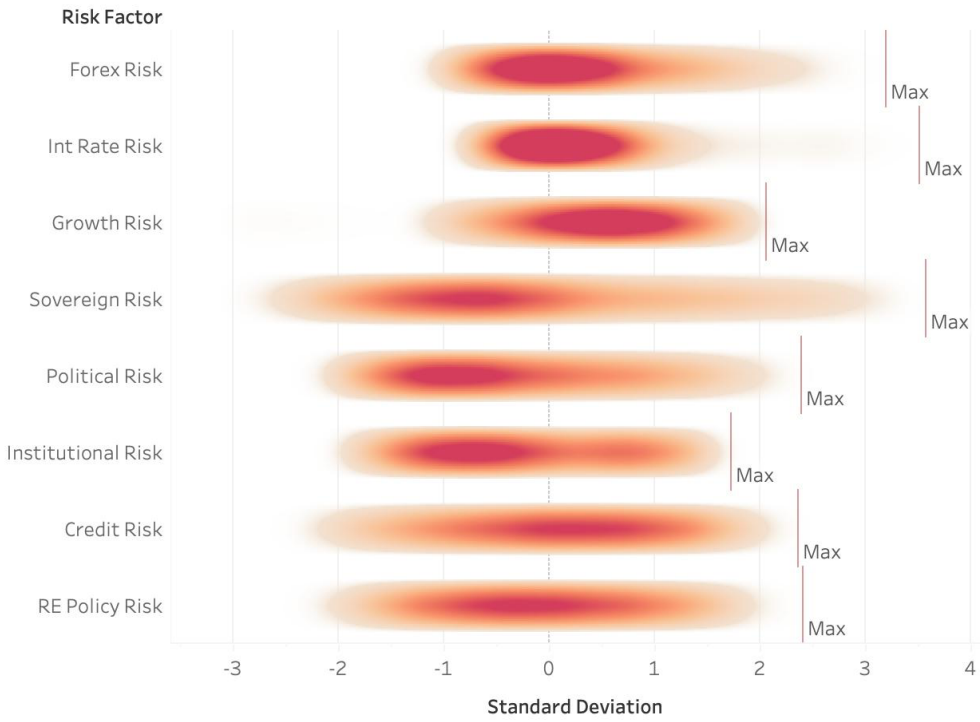


Figure 2: Distribution of different risks in the investible space. Positive values indicate higher risks. Stronger colours indicate a higher level of potential suitability at a particular level of risk based on past investments.

Interaction of Macro Risks

Beyond defining the frontiers of the investible space in terms of individual risks, the complex shape of the hypervolume as shown in Figure 1 highlights that investment decisions are not independently determined by individual risk levels. Alongside the non-linearity in the response of investment decisions to the levels of risk of distinct risk factors, there is a non-linear response to collective risk configurations. Different risk factors combine to form a risk landscape that ultimately determines the investment suitability of

macro environments. Risks balance, accentuate, correlate and combine with each other in distinct ways to produce non-linearity in investment outcomes (Figure 3).

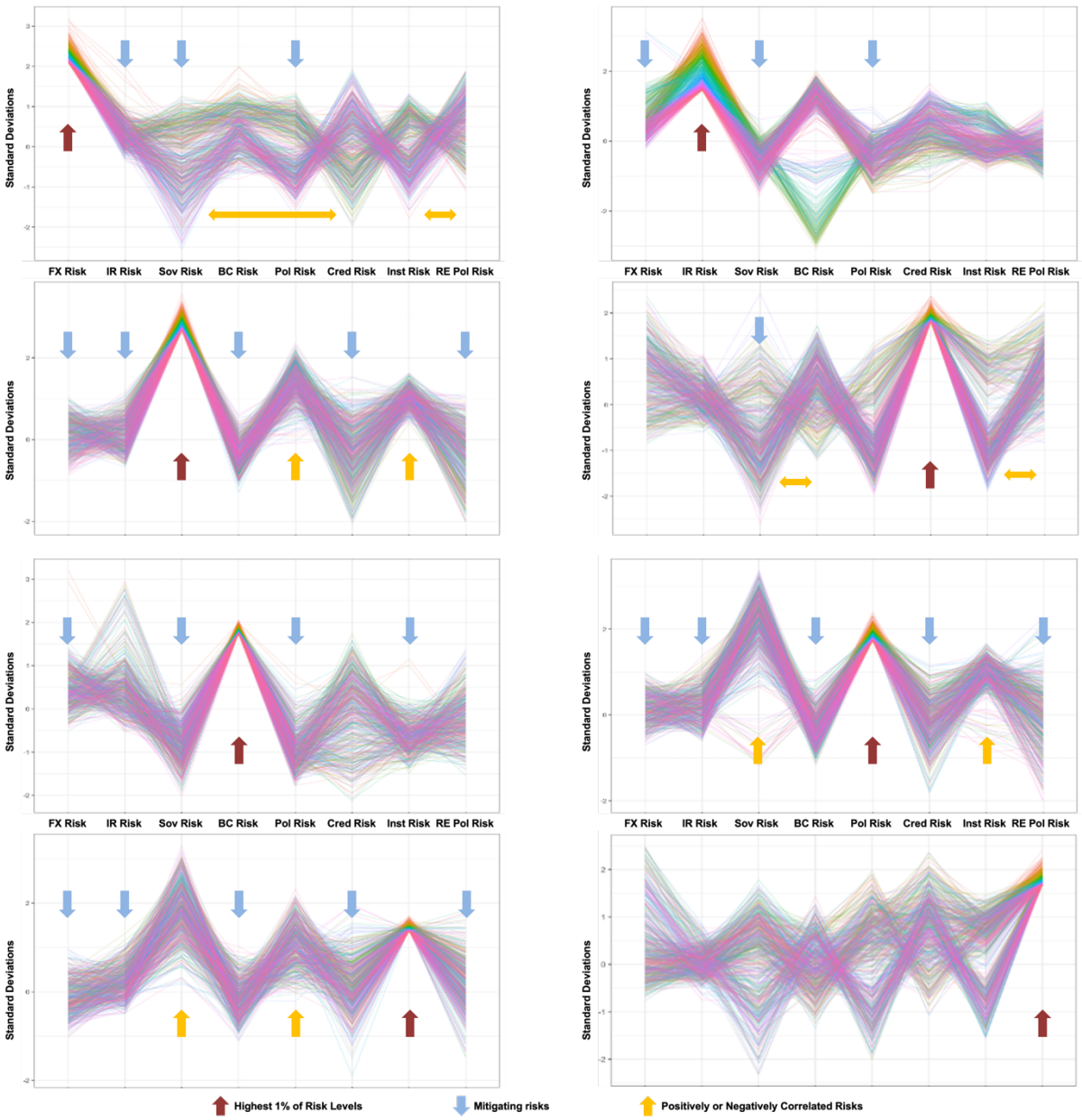


Figure 3: Suitable risk combinations, indicated by individual coloured lines across risk factors. Each panel shows the corresponding level of risks when one risk is very high – highest 1% values of one risk factor across all simulated points in the investible space.

Notable risk factor interactions include:

- Foreign exchange, interest rate and sovereign risks combine to create a higher risk environment for investments. High levels of any one of these risks are acceptable only if the others are relatively small.

- Sovereign, institutional and political risks are highly correlated. This suggests that countries often exhibit similar levels of these risks, despite them having distinct underlying risk drivers.
- High growth risk (i.e. low growth) environments need to feature low institutional, political, foreign exchange and sovereign risks to be suitable for investments – conditions typically observed in some HI countries. For most countries, a low growth or degrowth scenario significantly deters investments.
- High levels of sovereign credit risk are mitigated by low counterparty credit risk within the energy sector. A supportive renewable energy policy setup can further improve investment suitability by offsetting the impact of high institutional risk, which typically coexists with high sovereign risk. Conversely, high counterparty credit risk is acceptable alongside lower sovereign and institutional risks or in a high growth context.
- Given the impact of political risk on foreign exchange markets, high levels of both these risks combine to deter investments. An environment with high foreign exchange risk is investible only when political risk is very low, and given the high correlation, when institutional risk is also low.
- Some risks are additive in nature, neither balancing nor amplifying each other, due to differing underlying drivers. Meso-level risks, in particular, i.e. the risks specific to the renewable energy sector, are unconnected with some macroeconomic risks. For instance, foreign exchange risk, credit risk and renewable energy policy risk tend to be additive. Similarly, interest rate risks operate independently from credit and renewable energy policy risks.

Systemic Importance of Risk Factors

The presence of non-linear and joint impacts of individual risk factors on investment suitability requires a systemic measure to identify their impact on the high-dimensional investible space. This measure captures the contribution of individual macro risks to the overall volume of the investible space, and it can indicate to what extent the presence of a particular risk constrains the acceptable levels of other risks within a conducive investment environment. Smaller the contribution of a risk factor to the volume of the investible space, the fewer will be the risk combinations that will be conducive for investments and thereby greater constraints are imposed on the levels of other risks. To compute this, the SVM algorithm is used to construct a new hypervolume where an individual risk factor is removed as one of the dimensions. The ratio of the volume of the

original hypervolume relative to the resulting hypervolume provides a measure of the significance of the risk factor in expanding the hypervolume. And therefore, the inverse of this ratio indicates how small the contribution of the risk factor is in expanding the hypervolume, thereby constraining other risk factors and indicating its relative importance for investment suitability.

Roughly, this measure considers both the range of acceptable values for a particular risk, and the nature of its complex interactions with other risks. It thus goes beyond the traditional conception of risk analysis that takes a linear additive approach to risks and captures the interactions of macro risks as well as the non-linearity of investor response to risk combinations. Institutional risk, interest rate risk and foreign exchange risk emerge as the most impactful in creating a 'headroom' for other risks and thus mitigating these risks can significantly enhance overall investment suitability. However, risks that do not interact directly with a mitigated risk factor will still influence the investment environment independently. For instance, as counterparty credit risk and foreign exchange risk are largely additive both must be mitigated in conjunction to prevent the residual risk from rendering the environment unsuitable for investments.

Suitability of Investment Environments Worldwide

An investment suitability metric is derived using the probabilities generated from the KDE hypervolume estimation to evaluate the suitability of the macro investment environment across countries at a given point in time. For each country, individual risk factor levels are used as the coordinates for a test point and its distance is computed to each random point. The probability for the test point is then calculated as the average probability density across all random points weighted by the inverse of the distance of the random points from the test point. A suitability score for each point is then computed by normalising the weighted probability densities. Figure 4 shows the suitability score mapped across countries based on their macro environment in 2019.

Of the 121 countries for whom adequate data was available, the most conducive investment environments are predictably found in high-income countries, largely spread across North America, Europe and Asia Pacific, but also Chile, Panama and Uruguay in Latin America and Israel, Oman, Qatar and UAE in the Middle East. Overall, Europe & Central Asia and East Asia & Pacific have the largest proportion of countries considered

investible, followed by Latin America & Caribbean. In South Asia, only 2 countries – India and Sri Lanka have conducive macro environments – the other 5 are not evaluated as conducive. And within Sub-Saharan Africa, only 2 countries – Senegal and South Africa – are estimated to have investible environments for solar projects.

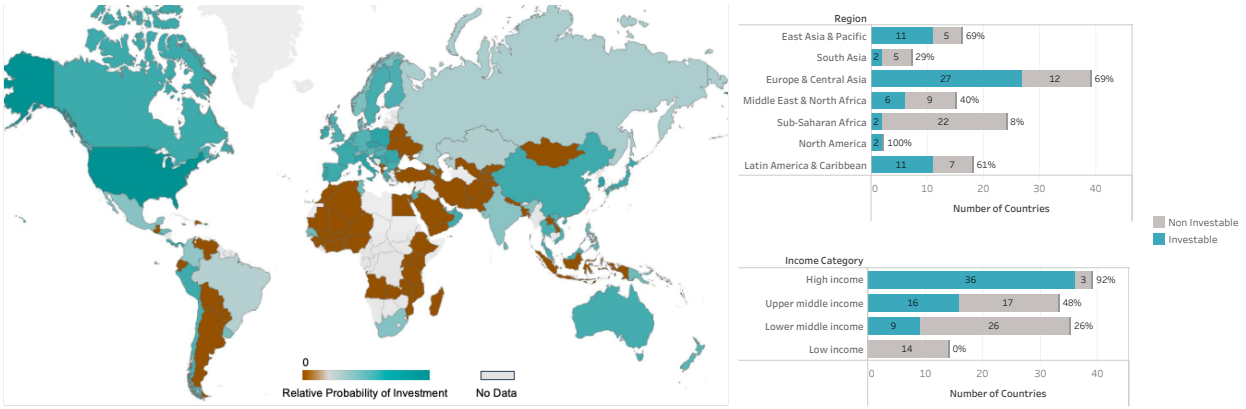


Figure 4: Left: Suitability of the macro investment environments of countries in 2019 for solar projects. Darker shades of blue indicate a greater relative probability of investment. Countries in brown are estimated to have a zero probability and the countries in light grey did not have adequate data available to make an estimation. Right: Classification of countries estimated to have investible or non-investible macro environment by region and income category based on World Bank classification.

Broadly, the probability of a country being considered investible closely corresponds to its income levels. Most High Income (HI) countries are classified as investible countries. The figure drops to just under half of Upper Middle Income (UMI) countries and roughly a quarter of Lower Middle Income countries (LMI). No Low Income (LI) countries are considered to have a conducive macro environment for solar investments. There are however regional variations. For instance, within Latin America & Caribbean, of the 7 countries considered non-investible, 6 are UMI countries, while 2 out of 3 LMI countries are classified as conducive. Nonetheless, the broad pattern of risk variation and investment suitability aligned with the income levels of countries indicates that a closer examination of risk frontiers by income groups might provide further insights.

Frontiers and Risk Factors across Country Groups

Different socio-economic contexts across countries exhibit distinctive risk profiles and interactions. High-income (HI), upper-middle-income (UMI), and lower-middle and low-income (LI) groups of countries display different ranges of acceptable risks (Figure 5).

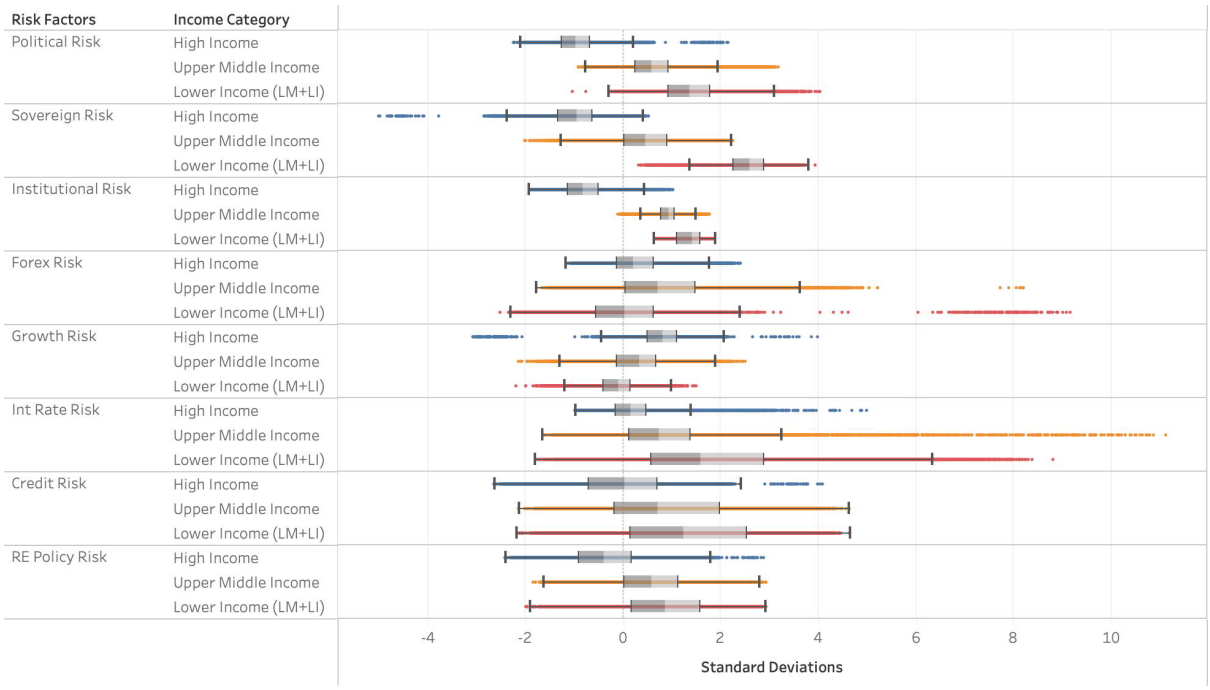


Figure 5: Distribution of different risks in the investible space across HI, UMI and LI groups of countries. The grey box indicates the centre of the distribution between 25th and 75th percentile values (inter-quartile range). The vertical tick-marks indicate the range of the distribution (1.5 x inter-quartile range). Risk levels beyond these may be considered extreme values.

Both UMI and LI groups are generally perceived to have higher levels of political, sovereign and institutional risks compared to HI countries, and this is reflected in the acceptable levels of these risks across the three groups. Institutional risk tolerance, however, narrows progressively across the groups, indicating that while UMI and LI countries feature higher institutional risks, only a narrow set of environments that fall within these strict limits will be considered suitable for investments. Given these inherent risk characteristics of UMI and LI countries, their investment suitability depends on the extent to which other risks are within acceptable bounds.

Suitable levels of foreign exchange risk are lowest in LI countries and even in the case of UMI countries, high levels of foreign exchange risk must be balanced by low levels of sovereign, political, institutional and credit risks. Similarly, high growth risk is generally acceptable only in HI and UMI countries with low sovereign and institutional risks alongside an otherwise medium- to low-risk environment. In contrast, LI countries struggle to attract investment in a low-growth environment in the absence of other compensating factors. On the other hand, a wider range of interest rate risk levels is acceptable in LI countries where they may be balanced by lower growth and foreign exchange risks. Counterparty credit and renewable energy policy risks also demonstrate wide levels of

acceptability across countries. But in LI countries, elevated levels of these risks will still require an otherwise low-risk environment to maintain investment suitability.

Discussion

The complexity of risk interactions in investment environments provides opportunities to mitigate and balance risks more effectively. Traditional risk analysis operates at an individual level of investment - asset, portfolio or investor - to understand the impact of risks on asset values. In contrast, a systemic approach to risks captures the broader response of the investment system to changes in the risk environment and incorporates the non-linearity in the response to individual risks and joint configurations of different risks. Foreign exchange, interest rate and sovereign credit risks, for instance, are systemically important financial risks that combine to create a non-linear impact on investment suitability. These therefore need be managed collectively to achieve a balance in their impact. It is technically possible to hedge these risks, for example through financial derivatives, insurance products, dollar denomination, sovereign guarantees, bilateral swaps or international debt guarantees. However, many of these options prove economically unviable, have capacity constraints or simply do not exist at the moment for long-term risk mitigation. This presents an opportunity to establish international mechanisms and create financial instruments that mitigate these risks more sustainably and efficiently. The impact that high foreign exchange risk creates on investment suitability, especially in countries with high sovereign credit risks, also highlights the importance of domestic local currency financing. Domestic mobilisation and development of local financial markets for renewable energy projects is imperative in economies with stable fundamentals and increasing economic development.

Strong economic growth and low levels of political and institutional risks can effectively counterbalance high levels of other risks but are challenging to achieve in the short run or through simple policy fixes. However, domestic energy policies can curtail counterparty credit risks and establish a favourable policy environment for renewable energy projects, which can combine to offset sovereign credit risks and counteract the effects of a weak institutional environment and higher political risks. In the case of MI and LI countries, creating conducive investment environments may thus require a combination of international mechanisms that can efficiently mitigate foreign exchange, interest rate and sovereign debt risks, coupled with domestic policies to curtail credit risks and provide

strong institutional support to the renewable energy sector. However, the broad benefits of improving governance standards, and thereby reducing institutional risks, on investment suitability need to be recognised as these create the maximum headroom for other risks.

The design of de-risking ‘packages' that involve mitigating multiple risks, however, must also consider the interactions between different risks. For instance, stable growing economies reduce the need for broad mitigation efforts and can instead focus on reducing key risks like foreign exchange risks. Conversely countries struggling with sluggish economic growth may require more comprehensive solutions or substantial public finance support than a focus on individual risk mitigation measures. The extent of mitigation needed for individual risks also depends on investor preferences for different risk configurations. Solutions can then be designed to target different acceptable combinations of risks based on the criteria of viability, affordability, efficiency and effectiveness. Adopting a systemic approach can thus yield cost-effective and scalable solutions by leveraging the non-linear interactions of risk factors and tailoring solutions to favour market-friendly risk configurations. This approach can be used to enhance investment environments in individual countries by strategically focusing on the specific risk interactions most relevant to their unique economic and institutional contexts, thereby maximizing their appeal to a range of investors.

References

Afanasyeva, S., Saari, J., Kalkofen, M., Partanen, J. and Pyrhönen, O. (2016) 'Technical, economic and uncertainty modelling of a wind farm project', *Energy Conversion and Management*, 107, pp. 22–33. Available at: https://doi.org/10.1016/j.enconman.2015.09.048.

Agliardi, E., Pinar, M. and Stengos, T. (2014) 'A sovereign risk index for the Eurozone based on stochastic dominance', *Finance Research Letters*, 11(4), pp. 375–384. Available at: https://doi.org/10.1016/j.frl.2014.07.002.

Aizenman, J., Jinjarak, Y. and Park, D. (2016) 'Fundamentals and Sovereign Risk of Emerging Markets', *Pacific Economic Review*, 21(2), pp. 151–177. Available at: https://doi.org/10.1111/1468-0106.12160.

Albertazzi, U., Ropele, T., Sene, G. and Signoretti, F.M. (2014) 'The impact of the sovereign debt crisis on the activity of Italian banks', *Journal of Banking & Finance*, 46, pp. 387–402. Available at: https://doi.org/10.1016/j.jbankfin.2014.05.005.

Ameli, N., Dessens, O., Winning, M., Cronin, J., Chenet, H., Drummond, P., Calzadilla, A., Anandarajah, G. and Grubb, M. (2021) 'Higher cost of finance exacerbates a climate investment trap in developing economies', *Nature Communications*, 12(1), p. 4046. Available at: https://doi.org/10.1038/s41467-021-24305-3.

Augustin, P., Boustanifar, H., Breckenfelder, J. and Schnitzler, J. (2018) 'Sovereign to Corporate Risk Spillovers', *Journal of Money, Credit and Banking*, 50(5), pp. 857–891. Available at: https://doi.org/10.1111/jmcb.12497.

Bhattacharya, A., Songwe, V., Soubeyran, E. and Stern, N. (2024) *Raising Ambition and Accelerating Delivery of Climate Finance*. London: Grantham Research Institute on Climate Change and the Environment, London School of Economics and Political Science. Available at: https://www.lse.ac.uk/granthaminstitute/publication/raising-ambition-and-accelerating-delivery-of-climate-finance/.

Blonder, B. (2023) 'hypervolume: High Dimensional Geometry, Set Operations, Projection, and Inference Using Kernel Density Estimation, Support Vector Machines, and Convex Hulls'. Available at: https://cran.r-project.org/web/packages/hypervolume/index.html.

Blonder, B., Lamanna, C., Violle, C. and Enquist, B.J. (2014) 'The *n* -dimensional hypervolume', *Global Ecology and Biogeography*, 23(5), pp. 595–609. Available at: https://doi.org/10.1111/geb.12146.

Blonder, B., Morrow, C.B., Maitner, B., Harris, D.J., Lamanna, C., Violle, C., Enquist, B.J. and Kerkhoff, A.J. (2018) 'New approaches for delineating *n* -dimensional hypervolumes', *Methods in Ecology and Evolution*. Edited by S. McMahon, 9(2), pp. 305–319. Available at: https://doi.org/10.1111/2041-210X.12865.

Canuto, O., Dos Santos, P.F.P. and De Sá Porto, P.C. (2012) 'MACROECONOMICS AND SOVEREIGN RISK RATINGS', *Journal of International Commerce, Economics and Policy*, 03(02), p. 1250011. Available at: https://doi.org/10.1142/S1793993312500111.

Cervantes, J., Garcia-Lamont, F., Rodríguez-Mazahua, L. and Lopez, A. (2020) 'A comprehensive survey on support vector machine classification: Applications, challenges and trends', *Neurocomputing*, 408, pp. 189–215. Available at: https://doi.org/10.1016/j.neucom.2019.10.118.

Chowdhury, A.R. (1993) 'Does exchange rate volatility depress trade flows? Evidence from error-correction models', *The review of economics and statistics*, pp. 700–706. Available at: https://doi.org/10.2307/2110025.

CPI (2023a) *Cost of Capital for Renewable Energy Investments in Developing Economies*. Available at: https://www.climatepolicyinitiative.org/wp-content/uploads/2023/06/Discussion-Paper-EM-Cost-of-Capital-for-RE-and-GCGF-FINAL-Jun-2023.pdf.

CPI (2023b) *Global Landscape of Climate Finance 2023*. Climate Policy Initiative. Available at: https://www.climatepolicyinitiative.org/wp-content/uploads/2023/11/Global-Landscape-of-Climate-Finance-2023.pdf.

Donastorg, A., Renukappa, S. and Suresh, S. (2017) 'Financing Renewable Energy Projects in Developing Countries: A Critical Review', *IOP Conference Series: Earth and Environmental Science*, 83, p. 012012. Available at: https://doi.org/10.1088/1755-1315/83/1/012012.

Egli, F. (2020) 'Renewable energy investment risk: An investigation of changes over time and the underlying drivers', *Energy Policy*, 140, p. 111428. Available at: https://doi.org/10.1016/j.enpol.2020.111428.

Emodi, N.V., Wade, B., Rekker, S. and Greig, C. (2022) 'A systematic review of barriers to greenfield investment in decarbonisation solutions', *Renewable and Sustainable Energy Reviews*, 165, p. 112586. Available at: https://doi.org/10.1016/j.rser.2022.112586.

ESMAP (2022) *Regulatory Indicators for Sustainable Energy (RISE)*. Washington, DC: World Bank. Available at: https://rise.esmap.org/data/files/reports/2022/RISE%202022%20Report%20Building%20Resilience.pdf.

Fuss, S., Szolgayova, J., Obersteiner, M. and Gusti, M. (2008) 'Investment under market and climate policy uncertainty', *Applied Energy*, 85(8), pp. 708–721. Available at: https://doi.org/10.1016/j.apenergy.2008.01.005.

Hastie, T., Tibshirani, R. and Friedman, J. (2008) *The elements of statistical learning: data mining, inference, and prediction*. 10. [print.], (corr. as of 4. print.). New York, NY: Springer (Springer series in statistics).

Hearst, M.A., Dumais, S.T., Osuna, E., Platt, J. and Scholkopf, B. (1998) 'Support vector machines', *IEEE Intelligent Systems and their Applications*, 13(4), pp. 18–28. Available at: https://doi.org/10.1109/5254.708428.

Hu, J., Harmsen, R., Crijns-Graus, W. and Worrell, E. (2018) 'Barriers to investment in utility-scale variable renewable electricity (VRE) generation projects', *Renewable Energy*, 121, pp. 730–744. Available at: https://doi.org/10.1016/j.renene.2018.01.092.

IEA (2024) *World Energy Outlook 2024*. Paris: IEA. Available at: https://www.iea.org/reports/world-energy-outlook-2024.

IMF (2023) *IMF Data*, *IMF*. Available at: https://www.imf.org/en/Data (Accessed: 3 January 2024).

Ioannou, A., Angus, A. and Brennan, F. (2017) 'Risk-based methods for sustainable energy system planning: A review', *Renewable and Sustainable Energy Reviews*, 74, pp. 602–615. Available at: https://doi.org/10.1016/j.rser.2017.02.082.

IRENA (2016) *Unlocking Renewable Energy Investment: The Role of Risk Mitigation and Structured Finance*. Abu Dhabi: International Renewable Energy Agency. Available at: https://www.irena.org/-/media/Files/IRENA/Agency/Publication/2016/IRENA_Risk_Mitigation_and_Structured_Finance_2016.pdf.

IRENA (2024) *Renewable Power Generation Costs in 2023*. Abu Dhabi: International Renewable Energy Agency. Available at: https://www.irena.org/-/media/Files/IRENA/Agency/Publication/2024/Sep/IRENA_Renewable_power_generation_costs_in_2023.pdf.

Kaufmann, D. and Kraay, A. (2023) 'Worldwide Governance Indicators'. Available at: www.govindicators.org (Accessed: 19 October 2023).

Kaufmann, D., Kraay, A. and Mastruzzi, M. (2010) *The Worldwide Governance Indicators: Methodology and Analytical Issues*. World Bank Policy Research Working Paper No. 5430. Available at: https://ssrn.com/abstract=1682130.

McLachlan, G.J., Lee, S.X. and Rathnayake, S.I. (2019) 'Finite Mixture Models', *Annual Review of Statistics and Its Application*, 6(1), pp. 355–378. Available at: https://doi.org/10.1146/annurev-statistics-031017-100325.

Nijsse, F.J.M.M., Mercure, J.-F., Ameli, N., Larosa, F., Kothari, S., Rickman, J., Vercoulen, P. and Pollitt, H. (2023) 'The momentum of the solar energy transition', *Nature Communications*, 14(1), p. 6542. Available at: https://doi.org/10.1038/s41467-023-41971-7.

Nissim, D. and Penman, S.H. (2003) 'The Association between Changes in Interest Rates, Earnings, and Equity Values*', *Contemporary Accounting Research*, 20(4), pp. 775–804. Available at: https://doi.org/10.1506/YKRX-HUQU-9V28-EA16.

Ouedraogo, N.S. (2019) 'Opportunities, Barriers and Issues with Renewable Energy Development in Africa: a Comprehensible Review', *Current Sustainable/Renewable Energy Reports*, 6(2), pp. 52–60. Available at: https://doi.org/10.1007/s40518-019-00130-7.

Pereira, E.J.D.S., Pinho, J.T., Galhardo, M.A.B. and Macêdo, W.N. (2014) 'Methodology of risk analysis by Monte Carlo Method applied to power generation with renewable energy', *Renewable Energy*, 69, pp. 347–355. Available at: https://doi.org/10.1016/j.renene.2014.03.054.

Persaud, A. (2023) *Unblocking the green transformation in developing countries with a partial foreign exchange guarantee*. Climate Policy Initiative. Available at:

https://www.climatepolicyinitiative.org/wp-content/uploads/2023/06/An-FX-Guarantee-Mechanism-for-the-Green-Transformation-in-Developing-Countries.pdf.

Popescu, A. and Rafael Smets, F. (2010) 'Uncertainty, Risk-taking, and the Business Cycle in Germany', *CESifo Economic Studies*, 56(4), pp. 596–626. Available at: https://doi.org/10.1093/cesifo/ifq013.

Raikar, S. and Adamson, S. (2020) 'Renewable project finance structures and risk allocation', in *Renewable Energy Finance*. Elsevier, pp. 55–66. Available at: https://doi.org/10.1016/B978-0-12-816441-9.00005-2.

Rampini, A.A. (2004) 'Entrepreneurial activity, risk, and the business cycle', *Journal of Monetary Economics*, 51(3), pp. 555–573. Available at: https://doi.org/10.1016/j.jmoneco.2003.06.003.

Rosenblum, H. and Strongin, S. (1983) 'Interest rate volatility in historical perspective', *Economic Perspectives*, 7(1), pp. 10–19. Available at: https://www.chicagofed.org/~/media/publications/economic-perspectives/1983/ep-jan-feb1983-part3-rosenblum-pdf.pdf.

Schölkopf, B., Williamson, R.C., Smola, A., Shawe-Taylor, J. and Platt, J. (1999) 'Support vector method for novelty detection', *Advances in neural information processing systems*, 12. Available at: https://proceedings.neurips.cc/paper/1999/hash/8725fb777f25776ffa9076e44fcfd776-Abstract.html.

Serenis, D. and Tsounis, N. (2012) 'A New Approach for Measuring Volatility of the Exchange rate', *Procedia Economics and Finance*, 1, pp. 374–382. Available at: https://doi.org/10.1016/S2212-5671(12)00043-3.

Silverman, B.W. (2018) *Density estimation for statistics and data analysis*. Routledge.

Songwe, V., Stern, N. and Bhattacharya, A. (2022) *Finance for climate action - Scaling up investment for climate and development*. London: Grantham Research Institute on Climate Change and the Environment, London School of Economics and Political Science. Available at: https://www.cgdev.org/sites/default/files/IHLEG-report-finance-for-climate-action.pdf.

Sosa-Padilla, C. (2018) 'Sovereign defaults and banking crises', *Journal of Monetary Economics*, 99, pp. 88–105. Available at: https://doi.org/10.1016/j.jmoneco.2018.07.004.

Steffen, B. (2020) 'Estimating the cost of capital for renewable energy projects', *Energy Economics*, 88, p. 104783. Available at: https://doi.org/10.1016/j.eneco.2020.104783.

Vernazza, D.R. and Nielsen, E.F. (2015) 'The Damaging Bias of Sovereign Ratings', *Economic Notes*, 44(2), pp. 361–408. Available at: https://doi.org/10.1111/ecno.12037.

Waissbein, O., Glemarec, Y., Bayraktar, H. and Schmidt, T.S. (2013) *Derisking Renewable Energy Investment. A Framework to Support Policymakers in Selecting Public Instruments to Promote Renewable Energy Investment in Developing Countries*. New York, NY: United Nations Development Programme. Available at: https://www.undp.org/publications/original-drei-report.

Weber, B. and Alfen, H.W. (2010) *Infrastructure as an Asset Class: Investment Strategies, Project Finance and PPP*. Hoboken: John Wiley & Sons. Available at: http://public.eblib.com/choice/publicfullrecord.aspx?p=564927 (Accessed: 26 December 2016).

Węglarczyk, S. (2018) 'Kernel density estimation and its application', *ITM Web of Conferences*. Edited by W. Zielinski, L. Kuchar, A. Michalski, and B. Kazmierczak, 23, p. 00037. Available at: https://doi.org/10.1051/itmconf/20182300037.

Yasmeen, R., Tao, R., Jie, W., Padda, I.U.H. and Shah, W.U.H. (2022) 'The repercussions of business cycles on renewable & non-renewable energy consumption structure: Evidence from OECD countries', *Renewable Energy*, 190, pp. 572–583. Available at: https://doi.org/10.1016/j.renene.2022.03.138.

Acknowledgements

The authors acknowledge funding from the Green Climate Fund under research contract no. GCF 023/018.

Competing Interests Statement

The authors declare no competing interests.

Appendix A: Macro Risks, Indicators and Data

This study evaluates eight macro risk factors that are described below:

Foreign Exchange Risk

Variability in the exchange rate of the domestic currency of the project country against foreign currencies can impact a project in various ways. Project returns may be reduced for equity investors of operational projects if the capital investment has been made in a foreign currency and the revenues are generated in the local currency. Any depreciation in the value of the local currency vis-à-vis the foreign currency will thus lead to lower payments for foreign investors. International debt financiers may be similarly impacted depending on the currency of the financing – local currency denominated debt will yield local currency returns which will lead to lower earnings in foreign currency and foreign currency denominated debt will lead to a deterioration of debt service capacity of the project company increasing credit risk. High variability in foreign exchange rates can also affect potential investments in upcoming projects where investors are unsure of project returns, which in turn will stifle foreign investments that are particularly crucial for developing countries pursuing rapid clean energy deployment. It can also increase costs for projects during the development phase if key inputs such as solar panels are imported and paid for in foreign currency. High exchange rate variability can also have secondary macroeconomic effects by impacting inflation, interest rates and trade flows, which can destabilise economies and impact their growth.

This study measures exchange risk volatility using the annualised value of the standard deviation across a 5-year moving window of the log returns of monthly exchange rates. This is a common measure used in economic studies and captures the medium-term volatility of exchange rates (Chowdhury, 1993; Serenis and Tsounis, 2012). Monthly values of the exchange rates of currencies against the International Monetary Fund's (IMF) Special Drawing Rights (SDR) are used to compute this volatility indicator (IMF, 2023).

$$EV_t = \left[\left({}^{1}/_{m}\right) \sum_{i=1}^{m} (log\ Q_{t-i+1} - log\ Q_{t-i})^2 \right]^{1/2}$$

Where:

EV_t is the historical exchange rate volatility at time *t*,

Q_t is the exchange rate at time *t*, and

m is the length of the computation window in months.

Interest Rate Risk

Movement in interest rates impacts projects directly through a change in interest payments on loans used to finance the project. This is because interest rates on loans are usually floating i.e. benchmarked against an inter-bank short-term interest rate throughout the lifetime of the loan (Weber and Alfen, 2010). An increase in reference interest rates leads to an increase in financing costs and reduces the project returns for equity investors even if the interest margin remains the same. Interest margin may itself change for future financing of the project based on prevalent economic and financing conditions as projects are usually financed multiple times through their life with different loans covering smaller time periods. Interest rate risk can further impact the value of the project and the corresponding equity through a change in discount rates, which are also linked to the risk-free interest rate (Nissim and Penman, 2003). In this way, interest rate volatility can affect the entire capital structure.

This study uses the annualised value of the standard deviation across a 2-year moving window of monthly changes in annual interest rates, again a measure consistent with existing economic literature which captures the effect of short-term volatility of interest rates (Rosenblum and Strongin, 1983). The interest rate indicator is one of money market interest rate, treasury bill rate or the central bank policy rate for each country, based on data availability, sourced from the IMF database (IMF, 2023).

$$IV_t = \left[\left(1/m\right) \sum_{i=1}^{m} (R_{t-i+1} - R_{t-i})^2 \right]^{1/2}$$

Where:

IV_t is the historical interest rate volatility at time *t,*

R_t is the interest rate in percentage points at time *t*, and

m is the length of the computation window in months.

Growth Risk

Cyclical movements in the broader economy of a country lead to fluctuations in energy demand due to changing production-consumption cycles and thus affect the prospects of renewable energy projects (Yasmeen *et al.*, 2022). Reduced energy demand during economic downturns may lead to projects losing out on revenue due to a demand-supply imbalance in the energy system that may require renewable energy projects to cut energy production. Additionally, business cycles have been found to increase economic uncertainty and financial risk premiums in the banking sector during downturns (Popescu and Rafael Smets, 2010). Increased risk aversion of investors may lead to credit curtailment in the banking system and a reduction in the willingness of project sponsors to bear project-specific risks (Rampini, 2004). Thus, negative turns in economic cycles will result in reduced financing for renewable projects, high financial costs for debt capital and a greater expected return on equity in the context of reduced demand for energy, which can have a significant impact on the prospects of the renewable energy sector.

This study uses the average quarter-on-quarter growth rate of the previous 4 quarters as an indicator of the short-term prospects of the economy using the data on real GDP in domestic currency and where unavailable the annual percentage growth in real GDP from the IMF database.

$$BCI_t = \left({}^{1}/_{4}\right) . \sum_{i=1}^{4} \frac{(GDP_{t-i-1} - GDP_{t-i-2})}{GDP_{t-i-2}}$$

Where:

BCI_t is the business cycle risk indicator at time *t,*

GDP_t is the real GDP in domestic currency at time *t.*

Sovereign Risk

The creditworthiness of the country's government where a project is located can have a substantial bearing on project returns and costs. A direct impact is through the contractual involvement of the government with the project through power purchase agreements, capacity market contracts, risk guarantees and other incentives or rebate schemes. Deterioration in the capacity of the government to meet its contractual obligations can lead to risks concerning the probability and timing of project cash flows. Further, an increase in the riskiness of the sovereign credit position affects the domestic banking sector which

typically holds a significant amount of government debt on its balance sheet to control the level of risk in its asset portfolio and meet reserve requirements. Uncertainty in the value of these assets leads the financial sector to increase risk premiums and decrease lending to maintain solvency, thereby affecting the availability of finance and increasing the financing costs for the project (Albertazzi *et al.*, 2014; Sosa-Padilla, 2018). Similarly, foreign currency flows to the country can be impacted due to the possibility of restrictions and illiquidity on foreign currency conversions starving the sector further of financing. In order to improve the debt repayment capacity and instil market confidence, governments may resort to fiscal actions that can increase taxation costs and decrease investments and aggerate demand in the economy (Augustin *et al.*, 2018). These actions will further reduce the profitability of renewable energy projects.

This study captures sovereign credit risk through a debt service coverage ratio defined as the gross debt position of the government divided by government revenue. This ratio indicates the current capacity of the government to service outstanding debt and has been found to be a significant indicator of sovereign risk in studies (Canuto, Dos Santos and De Sá Porto, 2012; Agliardi, Pinar and Stengos, 2014). The perception of sovereign risk is typically offset by the size of the economy as it indicates the capacity of the government to increase revenue generation through fiscal actions to make interest payments and debt repayments (Aizenman, Jinjarak and Park, 2016). The coverage ratio is therefore downscaled by the GDP per capita to account for the capacity of a country to raise further resources to pay its debt based on the strength of its economy. This scaled indicator has been compared with point-in-time sovereign risk ratings provided by S&P and performs well while avoiding the discrete and subjective nature of these ratings (Vernazza and Nielsen, 2015). The underlying data for the indicator is sourced from the IMF database.

$$SRI_t = \frac{GD_{t-1}}{R_{t-1}} \times \frac{1}{GDP_{t-1}}$$

Where:

SRI_t is the sovereign credit risk indicator at time *t,*

GD_t is the gross debt at time *t*,

R_t is the revenue at time *t*,

GDP_t is the real GDP per capita in domestic currency at time *t.*

Offtaker Credit Risk

Most renewable projects sign short- or long-term power purchase agreements (PPA) with major power utilities and in some cases with power traders or large-scale consumers to assure prices and demand for the generated electricity. They are therefore exposed to credit risk arising from a weakened credit position of the counterparty. Any delay or default in payments affects revenues, returns and solvency of the project.

This study uses the counterparty risk score from the RISE indicators produced by the Energy Sector Management Assistance Program and the World Bank (ESMAP, 2022). This indicator captures offtaker entity creditworthiness, payment risk mitigation measures at the entity and PPA level, and transparency and reliability in the reporting of financial and technical performance metrics.

Political Risk

Since renewable energy projects are long-term investments, they are exposed to risks emanating from the stability of the political system. An unstable political system may lead to changes in legislation, nationalisation of energy infrastructure, seizure and expropriation of operational assets, withdrawal of permits and incentives and shifting energy policies that result in a sudden deterioration of asset values. Further, political violence caused by internal strife or wider geopolitical conflict can cause severe disruption to projects. It can lead to damages to project equipment, transmission lines and end-user infrastructure leading to physical and revenue losses. The abrupt nature of turbulent events makes these risks and the scale of associated damages difficult to estimate.

This study uses the Political Stability and Absence of Violence/Terrorism indicator from Worldwide Governance Indicators compiled by the World Bank to measure political risk in countries (Kaufmann and Kraay, 2023). This indicator aggregates data from various credible think tanks, and non-governmental and international organisations, which regularly provide data indicating the likelihood of instability and adverse political events, violence and terrorism across countries. Normalised data across disparate sources is aggregated using a uniform components model that results in a score ranging from -2.5 to 2.5 spread across a standard normal distribution with a zero mean and standard deviation of one (Kaufmann, Kraay and Mastruzzi, 2010). Higher indicator values indicate better political environments.

Institutional Risks

Institutional risks are created due to shortcomings in the governance, legal and regulatory environment of the project country and can affect the project from its development to its long operational life and even decommissioning stages. A poor institutional environment comprises policy uncertainties and abrupt changes, delays in policy implementation, ad hoc bureaucratic hurdles, difficulties in dealing with regulators, onerous permit requirements, slow speed of dispute resolution, insufficient legal recourse and corruption. These conditions create additional overheads, longer gestation periods, contingent liabilities and volatility in project returns.

This study captures the quality of institutions in a country through the aggregation of four indicators from the Worldwide Governance Indicators compiled by the World Bank: Government Effectiveness, Regulatory Quality, Rule of Law and Control of Corruption. Similar to the indicator on Political Stability and Absence of Violence/Terrorism, these individual indicators are compiled through the aggregation of the assessments of various organisations and modelled into a score between -2.5 to 2.5 spread across a standard normal distribution with mean zero and standard deviation of one. The indicator for institutional risk is then a simple sum of values across these four indicators and inherits the normal properties of the individual indicators, where the mean of the distribution is the sum of individual indicator means and the variance is a sum of individual variances.

Renewable Energy Policy Risks

Uncertainty in policies designed for the renewable energy sector has a direct impact on renewable energy investment. Altering subsidies and incentives, tariffs and taxes on imports, legal requirements for setting up projects, permit regulations, grid connection costs, energy market design, merit-order changes, curtailment payments et cetera, all change the costs, revenues and cashflows thereby affecting financing costs and project returns. Any retrospective changes to policy elements affect operational projects and can reduce investor returns. Both renewable energy policy uncertainty and policies that favour fossil-fuel projects and preserve existing infrastructure deter investment in renewables.

This study uses the aggregate Renewable Energy indicator from the RISE indicators produced by the Energy Sector Management Assistance Program and the World Bank. This metric captures the various elements of the policy and regulatory regime that are important for mobilising renewable energy investments. It measures the suitability of the policy environment by compiling sub-indicators that assess the legal framework for renewable energy expansion, long-term planning for the penetration of renewable energy in the energy system, financial and regulatory support for renewable energy including grid access and priority dispatch, the development of auction markets and support for small-scale producers, the ease and flexibility of network connection, renewables integration and usage, and the extent of carbon emissions monitoring and pricing. Individual scores across these sub-indicators are averaged to obtain country-level indicators at each time period.

Appendix B: Algorithms for Hypervolume Estimation

Gaussian Kernel Density Estimation (KDE)

KDE is a non-parametric method to estimate the probability density function of a random variable from a finite data sample by using a kernel function to weigh data points (Hastie, Tibshirani and Friedman, 2008). It thus avoids making assumptions about the underlying population distribution by learning the functional form from observed data. KDE can be considered as "a sum of bumps" located at the observed data points with the shape of the bump determined by the kernel (or weighing) function *K* and the width by a smoothing (or bandwidth) parameter *h* (Silverman, 2018).

$$\hat{f}(x) = \frac{1}{nh} \sum_{i=1}^{n} K\left(\frac{x - X_i}{h}\right)$$

The kernel function is non-negative and bounded for all $x \in R$, and satisfies the condition:

$$\int_{-\infty}^{\infty} K(x)dx = 1$$

It thus functions as a probability distribution function. For a symmetrical kernel function, the exact shape of the function has been found to have little effect on the estimation of the probability density function (Silverman, 2018). Further, since the KDE estimator $\hat{f}(x)$ is an additive function of individual kernel functions, it will itself be a probability distribution function and inherit the properties of the kernel function such as continuity and differentiability. Thus, a Gaussian kernel function is advantageous as it provides a smooth output and is computationally fast (Węglarczyk, 2018). The smoothing or bandwidth parameter, *h*, on the other hand, has a larger bearing on the estimated probability density function – a low value results in a jagged shape of the function where a large quantity of individual detail and variation is captured whereas a high value results in over-smoothing, which may ignore important details in observed data. A standardised approach is therefore desirable to estimate a probability density function that is closer to the true density function. When a Gaussian kernel function is used, a simple estimator suggested by Silverman (2018) provides a good fit for a wide range of true density functions with minimal computation cost.

For estimating the hypervolume function, a Gaussian kernel function is used to generate a padded region around an input data point, with the distance along each axis controlled

by an individual bandwidth parameter. This region represents the potential set of points that may be included in the hypervolume with a probability defined by the Gaussian kernel function. Each of these Gaussian functions is centred at a data point and the hypervolume function is defined as a mixture density of these individual Gaussian kernel functions (McLachlan, Lee and Rathnayake, 2019). This hypervolume function assigns values to sample points based on their geometric proximity to input data points so that points closest to the input data points have the highest values and the function value decays asymptotically to zero for the farthest points.

There are three key tuning parameters for using the Gaussian KDE to estimate hypervolumes: the bandwidth (*h*) that controls the padding around each data point is set using the Silverman's estimator (2018) which is a Gaussian approximation that minimises the mean integrated squared error of the estimated distribution; the number of standard deviations (*sd.count*) of each axis that multiplied by the bandwidth defines the edge of hyperelliptical samples used for hypervolume estimation, with higher values leading to more accurate estimates over a larger region; and the probability threshold of the kernel density (*p*) that provides a threshold value for the hypervolume function for inclusion of points in the hypervolume.

One-Class Support Vector Machine (SVM)

SVMs are high-performance supervised learning algorithms that are widely used for classification problems with labelled data (Hearst *et al.*, 1998). These algorithms separate data into *n* different classes by finding the optimal *(n-1)* dimension hyperplane between data points that achieve the maximum margin i.e. a high degree of separation between them. A high level of margin indicates the maximum distance between boundary points, called support vectors, and ensures a low level of error. The hyperplane serves as a decision function, which once learned from existing data can be used to classify new data points into different groups. In the case of difficult classification problems, non-linear separation planes can be found by using kernel functions to transform the data points into a high-dimensional feature space that makes it easier to find the hyperplanes and separate the data into different classes (Cervantes *et al.*, 2020). In the case where clear separation between classes is difficult, which is common in real-world data, a loss function is used to map the distance of a point from the margin and is minimised to correctly classify as many points as possible while maintaining a large margin of separation. SVMs have

also been extended to a one-class case where the algorithm learns a decision function that defines a class boundary using observed data and can classify a new data point as a similar or novel/outlier compared to the observed set (Schölkopf *et al.*, 1999).

A similar one-class SVM algorithm is used to delineate hypervolumes. It learns a hypervolume function from presence-only input data to identify regions of hyperspace that should be included in the hypervolume by making binary inclusion/exclusion predictions on sampled data points. Gaussian radial basis functions are chosen as kernel functions. These are commonly used functional forms and yield non-linear classification hyper-planes and consequently complicated hypervolume shapes. The hypervolume function is estimated as a weighted sum of multivariate radial basis functions centred on input data points. The weights are determined using an optimisation algorithm that assigns non-zero weights only to data points closest to the hypervolume edge which are called support vectors. This algorithm also determines an optimal threshold value of the hypervolume function such that only points with function values greater than the threshold are included in the hypervolume.

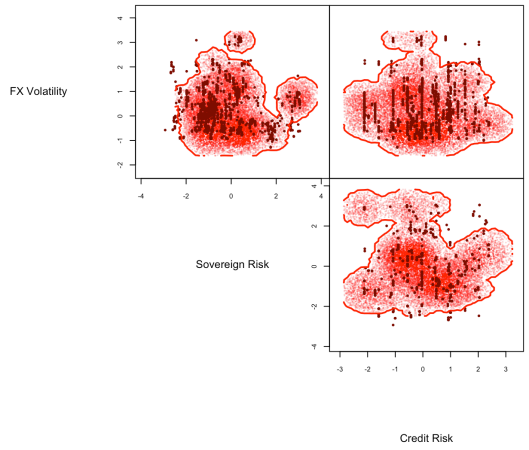
Two SVM tuning parameters are key for hypervolume estimation: the gamma (γ) parameter is used to compute the width of the radial basis functions and controls the distance of influence of an individual point such that low values lead to higher influences and simpler wraps around the data, and nu (ν) is a regularisation parameter that captures the trade-off between accuracy and over-fitting by controlling the permitted level of misclassification so that lower values lead to a tighter fit. The values of these parameters are application-specific and determine the level of smoothness and detail of the hypervolume shape. Like the KDE method, the set of random points that are evaluated using the estimated hypervolume function is determined by using hyperelliptical sampling to yield an efficient search space close to the data points. But the hyperellipses are centered only at the points identified as support vectors during hypervolume function estimation i.e. only the points identified to be near the hypervolume edge and stretch out to the maximal distance that would still yield a positive outcome.

Appendix C: Sensitivity Analysis for Hypervolume Estimation

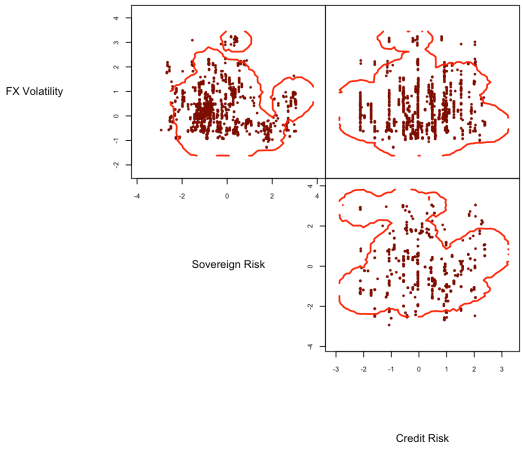
KDE Estimation

Model setup: Three variables with values filtered at the 99th percentile are input as unique values and densities.

<u>Default parameters:</u>



With random points



Without random points

Volume: 49.46

Random point density: 309.92

Number of random points: 15,327

Parameters:

kde.bandwidth: 0.2847309 0.4085848 0.3677141

kde.method: silverman

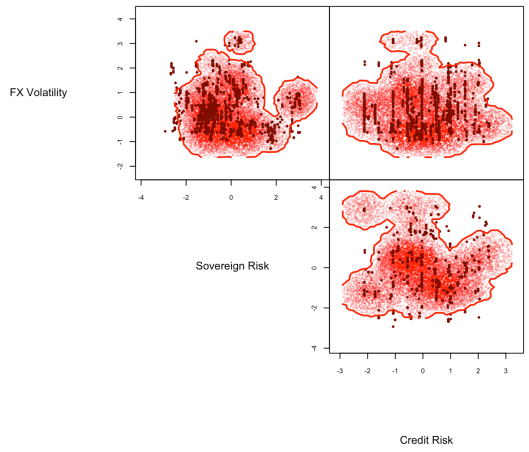
samples.per.point: 29

sd.count: 3

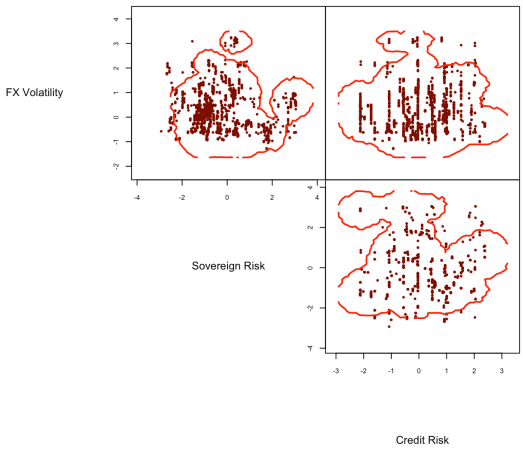
quantile.requested: 0.95

quantile.requested.type: probability

Increasing the number of random points per data point:



With random points



Without random points

Volume: 49.00

Random point density: 1070.58

Number of random points: 52,455

Parameters:

kde.bandwidth: 0.2847309 0.4085848 0.3677141

kde.method: silverman

samples.per.point: 100

sd.count: 3

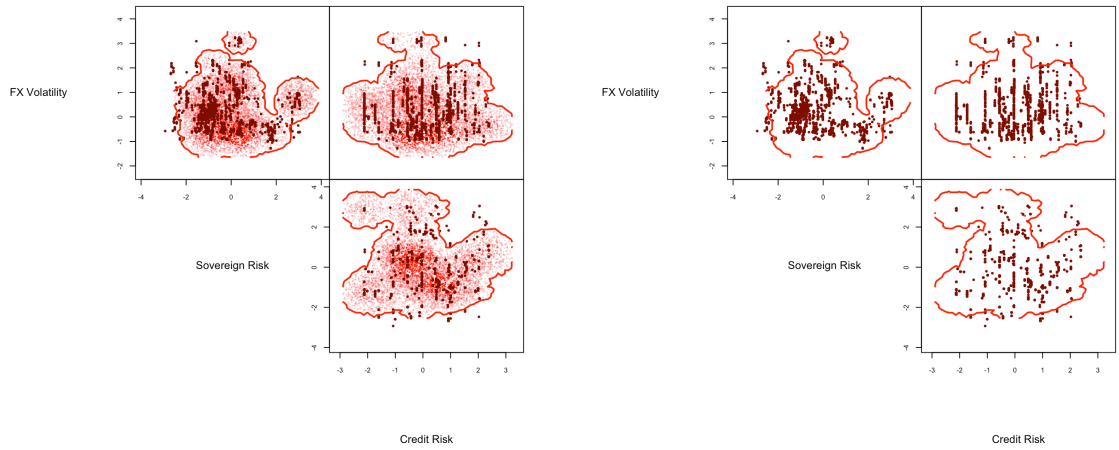
quantile.requested: 0.95

quantile.requested.type: probability

Impact:

An increase in the density of random points per data point being evaluated leads to a more precise delineation of boundaries and a minor reduction in the volume of the hypershape. However, *the computation time increases substantially and thus needs to be balanced against greater accuracy*.

Increasing the number of standard deviations of the hyperelliptical kernel i.e. the distance of the hyperelliptical region:



Volume: 50.13

Random point density: 126.02

Number of random points: 6,318

Parameters:

kde.bandwidth: 0.2847309 0.4085848 0.3677141

kde.method: silverman

samples.per.point: 29

sd.count: 6

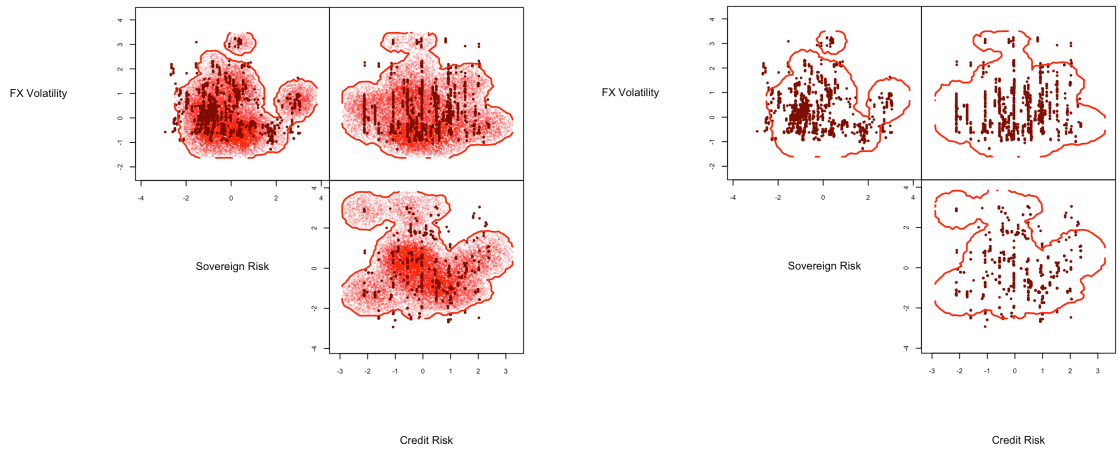
quantile.requested: 0.95

quantile.requested.type: probability

Impact:

An increase in the region of the hyperspace being evaluated leads to greater sampling of regions away from the data points resulting in a small increase in volume. *Increasing this parameter similarly increases the computation cost for modest gains in accuracy of the contour.*

Increasing both the number of random points per data point and the number of standard deviations of the hyperelliptical kernel



Volume: 48.89

Random point density: 1,303.59

Number of random points: 63,730

Parameters:

kde.bandwidth: 0.2847309 0.4085848 0.3677141

kde.method: silverman

samples.per.point: 300

sd.count: 6

quantile.requested: 0.95

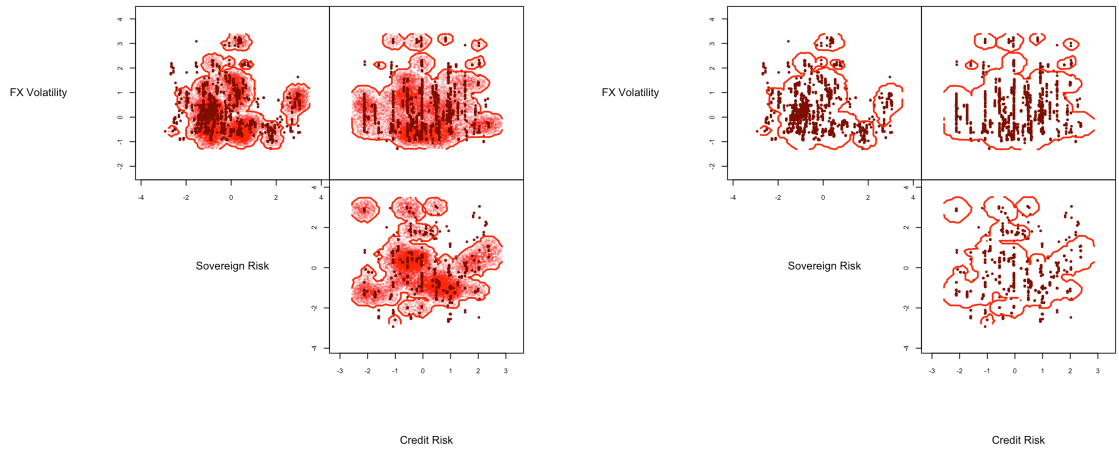
quantile.requested.type: probability

Impact:

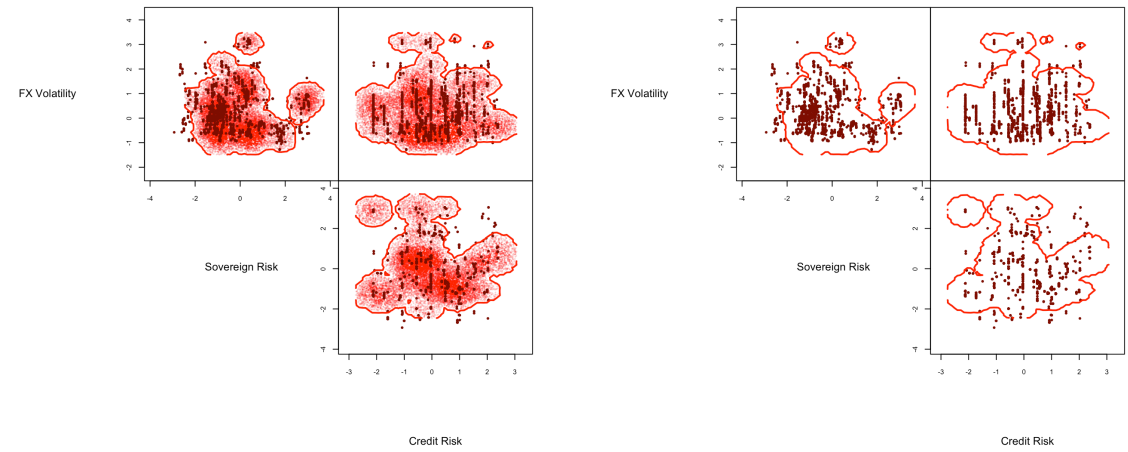
With a greater proportion of random points per data point and an expanded search area, the precision of the shape is greater resulting in smoother contour lines. However, the volume estimate remains close to the one generated by default parameters. Overall, it is observed that the default parameterisation generates a stable estimate of the volume of the hypershape. *An increase in the number of random points and the number of standard deviations may be employed to achieve smoother contour lines.*

Sensitivity of the Bandwidth parameter

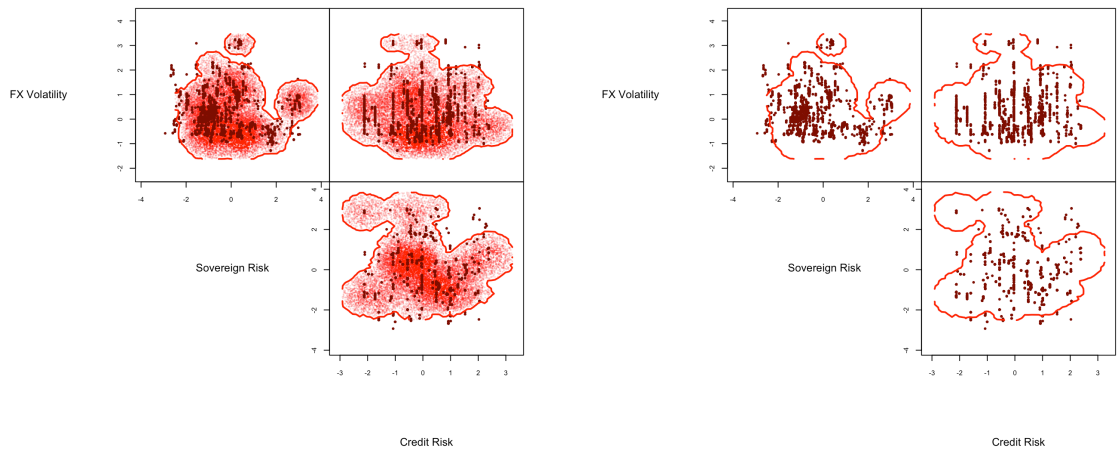
Scaling the Silverman bandwidth estimate by 0.5:



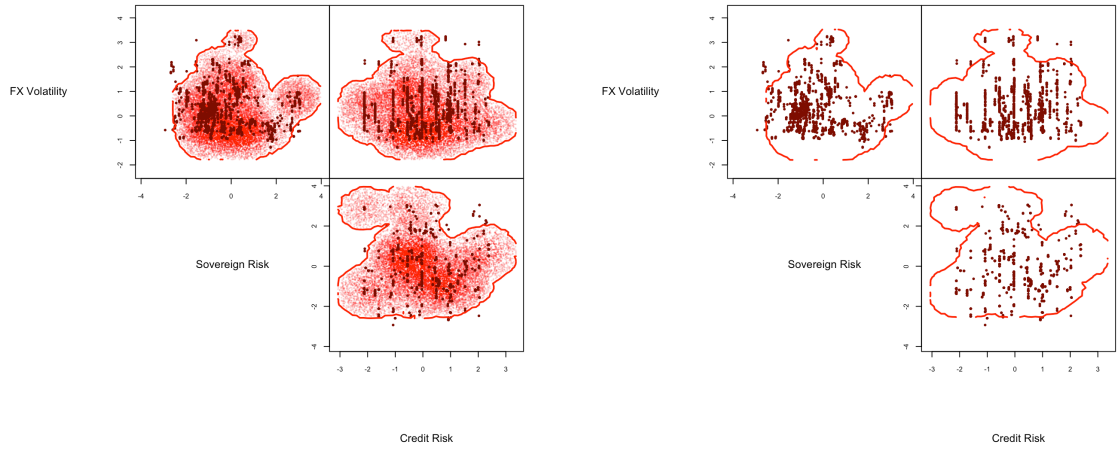
Scaling the Silverman bandwidth estimate by 0.75:



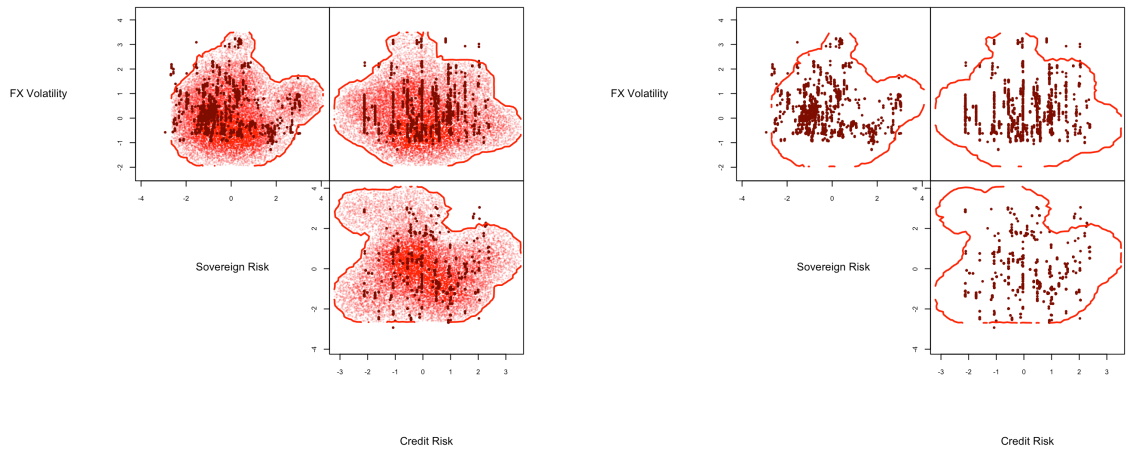
Default - Silverman bandwidth estimate:



Scaling the Silverman bandwidth estimate by 1.25:



Scaling the Silverman bandwidth estimate by 1.5:



Comparison:

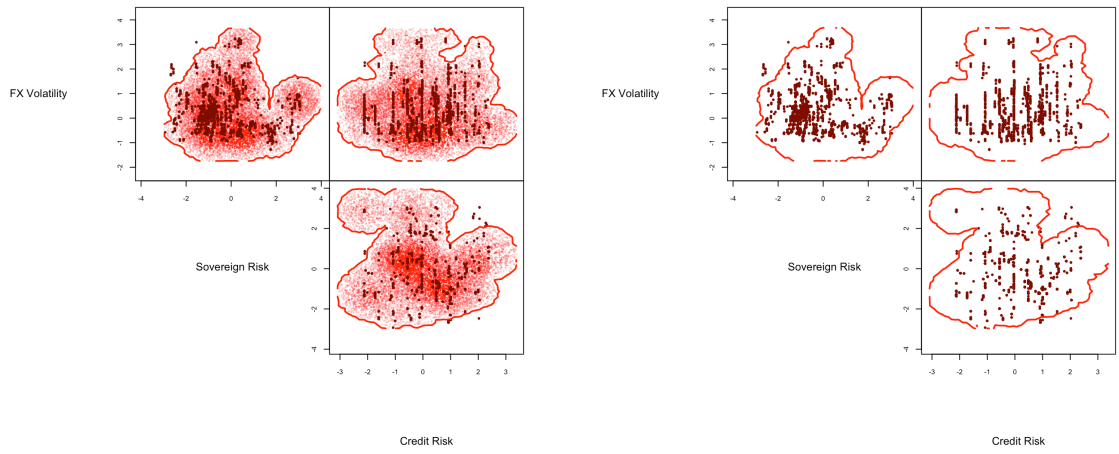
	SE*0.5	SE*0.75	SE	SE*1.25	SE*1.5
Volume	17.37	33.17	49.02	67.35	84.22
Random Point Density	2,572.35	1,513.41	1,070.41	815.29	645.75
Random Points	44,691	50,204	52,467	54,908	54,382
Bandwidth	0.14, 0.20, 0.18	0.21, 0.31, 0.28	0.28, 0.41, 0.37	0.36, 0.51, 0.50	0.43, 0.61, 0.55
Samples per point	100	100	100	100	100
No of SD	3	3	3	3	3

Impact:

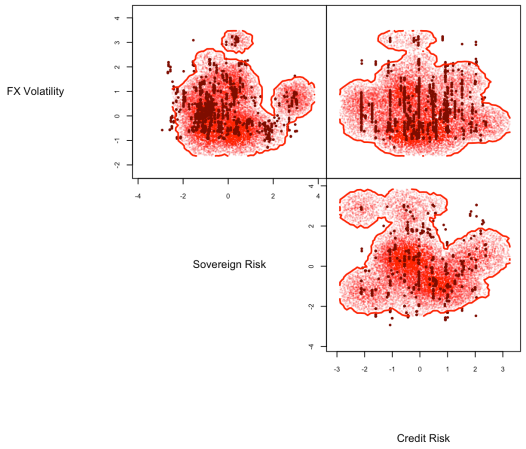
Varying the bandwidth parameter impacts the identification of a coherent hypervolume. Lower values of the parameter results in smaller hyperelliptical kernels whereby only random points within close proximity of existing data points are considered as suitable for inclusion within the hypervolume, given a probability threshold. This results in fragmented islands of hyperspace and holes in the geometric object. On the other hand, relatively higher values lead to large parts of the hyperspace to be included in the hypervolume as the probability spreads out to sparser regions. The inclusion of low-density areas of the hyperspace may thus lead to false identification of regions that are suitable. *Overall, the Silverman estimate provides a good balance between formation of discontinuous shapes and overfitting of the hypervolume across all data points.*

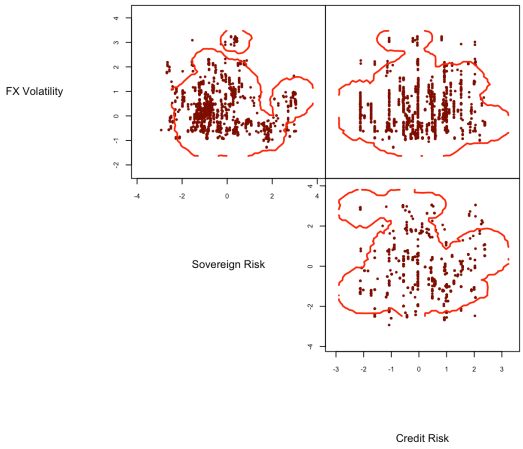
<u>Sensitivity of Threshold Parameter</u>

Threshold Quantile: 99%

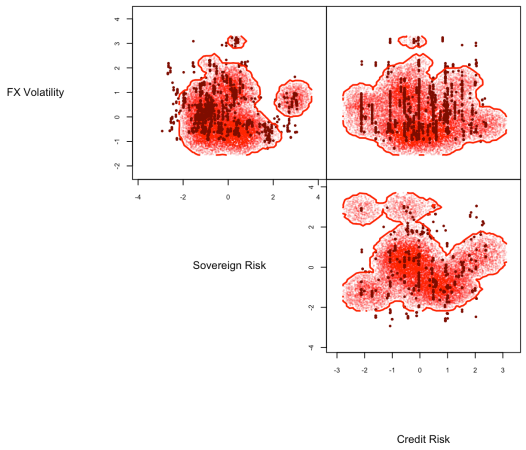


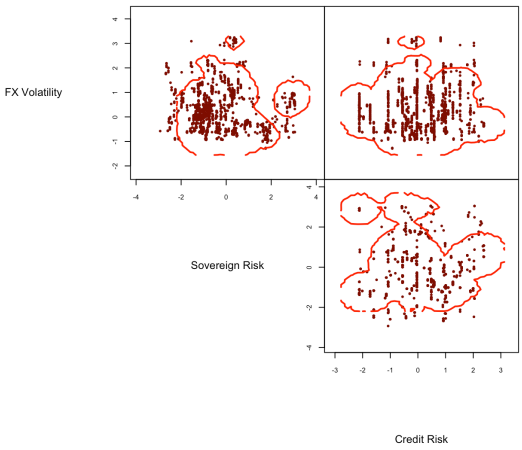
Threshold Quantile: 95%



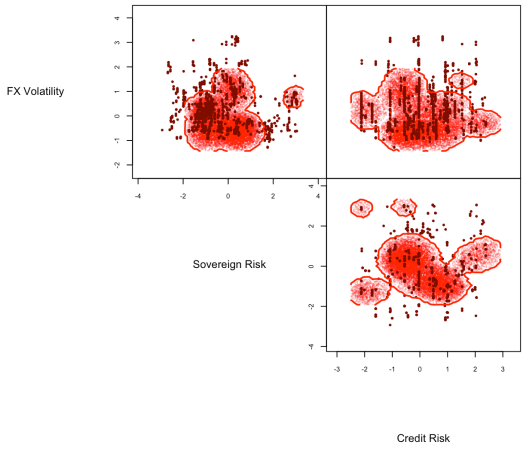


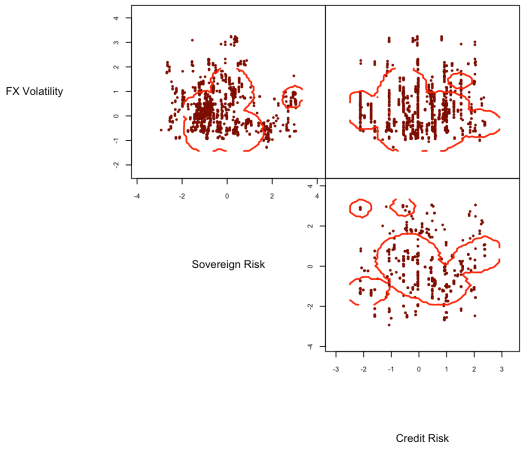
Threshold Quantile: 90%



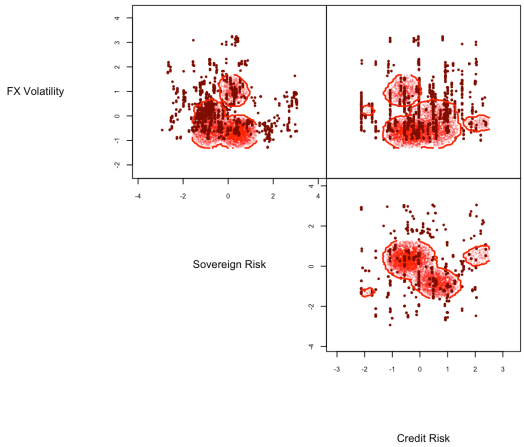


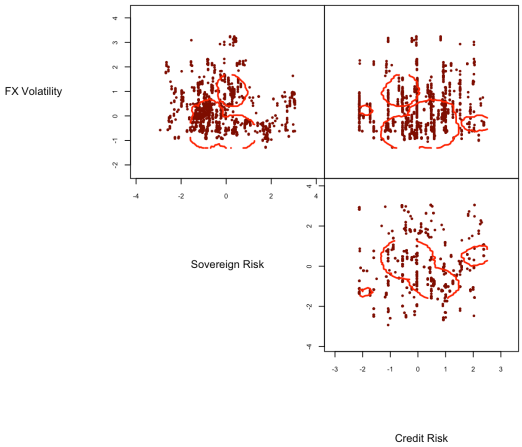
Threshold Quantile: 75%





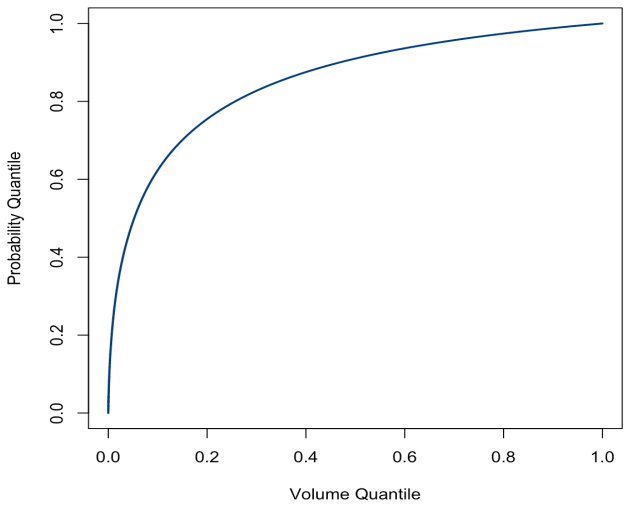
Threshold Quantile: 50%





Comparison:

	99%	95%	90%	75%	50%
Volume	74.85	48.97	34.78	16.19	5.72
Random Point Density	752.17	751.82	751.16	751.24	751.93
Random Points	56,297	36,817	26,128	12,109	4,299
Bandwidth	0.28, 0.41, 0.37	0.28, 0.41, 0.37	0.28, 0.41, 0.37	0.28, 0.41, 0.37	0.28, 0.41, 0.37
Samples per point	100	100	100	100	100
No of SD	4	4	4	4	4



Impact:
Higher levels of the threshold quantile parameter increase the volume of the hypershape but increasingly it occupies sparser regions of the hyperspace with few data points, e.g. the hypershape that covers 99% of the estimated probability density. *The default level of the parameter at 95% seems to perform reasonably well*, alongside the 90% threshold. Lower levels of the threshold quantile, such as the 75%, may be useful though for identifying the core region of the hypervolume with the highest density of data points.

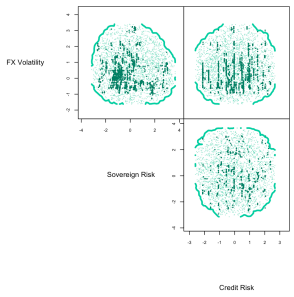
SVM Estimation
Model setup: Three variables with values filtered at the 99th percentile are input as unique values. The samples per point parameter is set at 100 to reduce computational time and resources.

Impact of parameter (ν,γ) values
The ν parameter controls the trade-off between acceptable estimation errors and overfitting. Very low values of the parameter, for instance at the default value of 0.01, includes most of the data points and leads to a hypervolume where there are areas with sparse random point density. The default value is thus found to result in a shape that is too expansive thereby making it difficult to delineate a precise contour implied by the data (below). *This is therefore altered to 0.1 which provides a good balance of tight fit around the data while limiting training errors.*

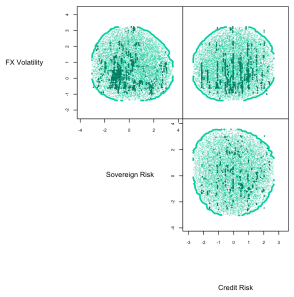
The γ parameter on the other hand controls the inverse distance of influence that a data point has on hypervolume boundary estimation and thus controls its smoothness/tightness around data values. Small values thus lead to larger influences and smooth broad wraps whereas high values result in tighter wraps that get noisier as the value is increased (below)*. The default value of the γ parameter works well overall for hypervolume delineation balancing smoothness with precision.* Smaller values lead to a loss of shape whereas higher values result in jagged and discontinuous shapes that are not suited for the goals of this research.

Summary Results:

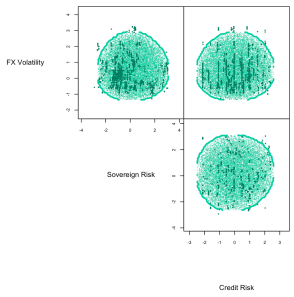
ν=0.01, γ=0.1



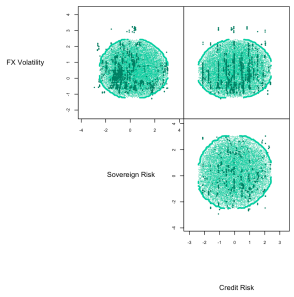
ν=0.05, γ=0.1



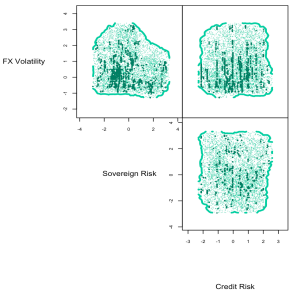
ν=0.1, γ=0.1



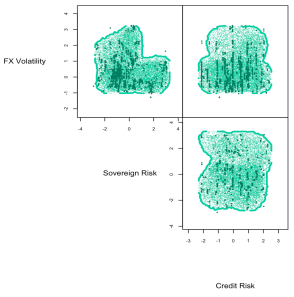
ν=0.2, γ=0.1



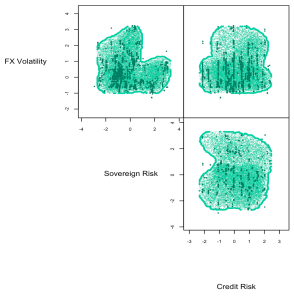
ν=0.01, γ=0.5



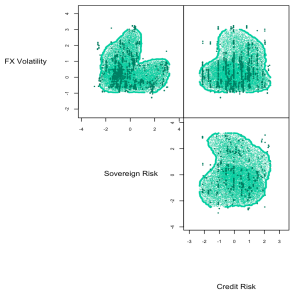
ν=0.05, γ=0.5



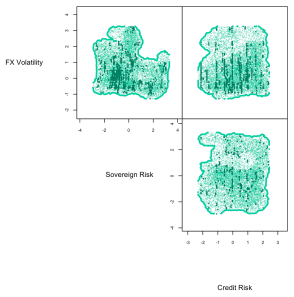
ν=0.1, γ=0.5



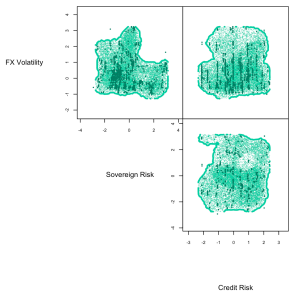
ν=0.2, γ=0.5



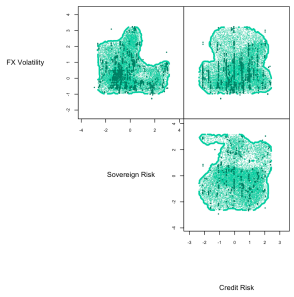
ν=0.01, γ=1



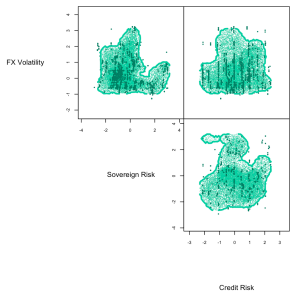
ν=0.05, γ=1



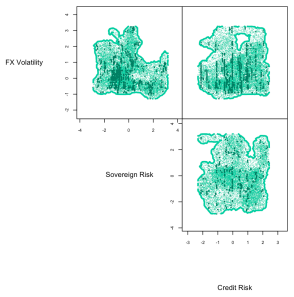
ν=0.1, γ=1



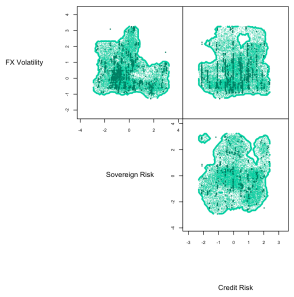
ν=0.2, γ=1



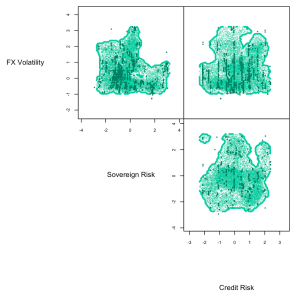
ν=0.01, γ=1.5



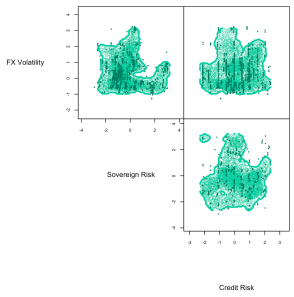
ν=0.05, γ=1.5



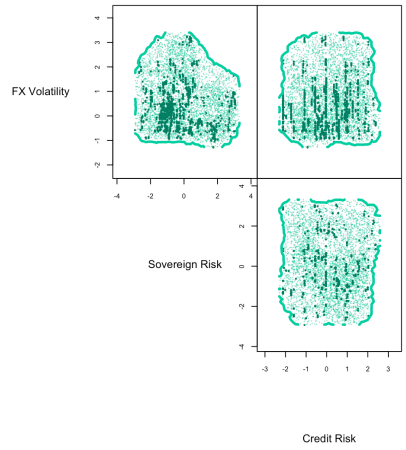
ν=0.1, γ=1.5

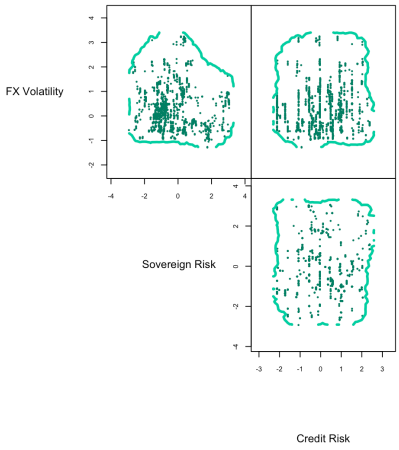


ν=0.2, γ=1.5



Default parameter values: ν=0.01, γ=0.5





Volume: 66.418064

Random point density: 67.752653

Number of random points: 4500

Parameters:

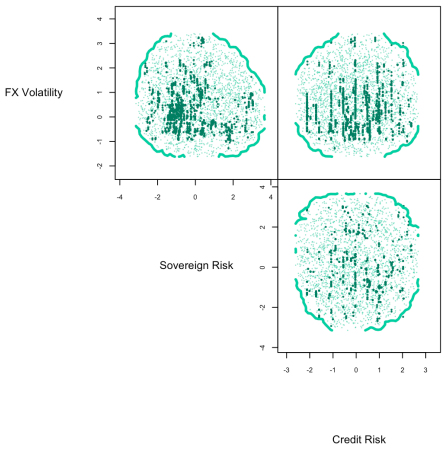
svm.nu: 0.01

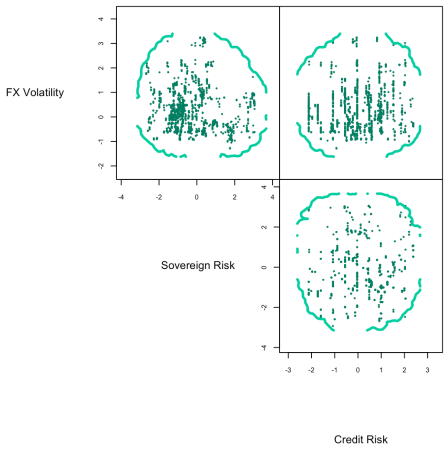
svm.gamma: 0.5

samples.per.point: 100

Exploring ν, γ values

ν=0.01, γ=0.1





Volume: 105.703575

Random point density: 21.758961

Number of random points: 2300

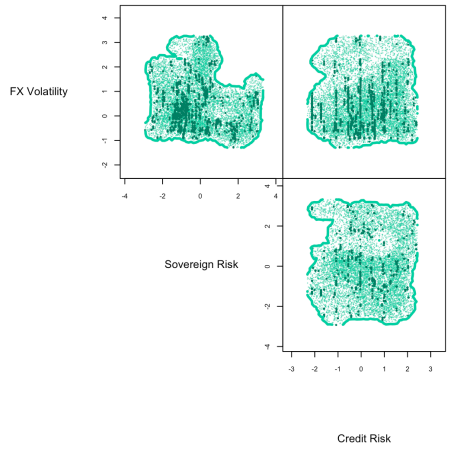
Parameters:

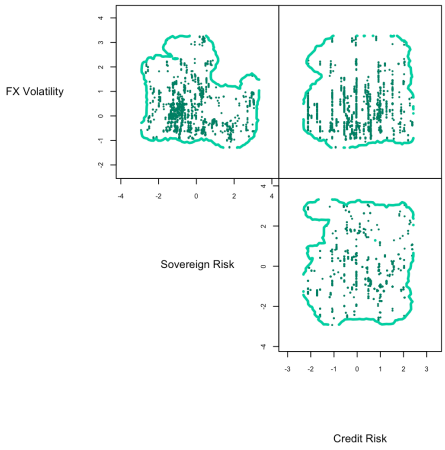
svm.nu: 0.01

svm.gamma: 0.1

samples.per.point: 100

ν=0.01, γ=1





Volume: 45.290087

Random point density: 209.758928

Number of random points: 9500

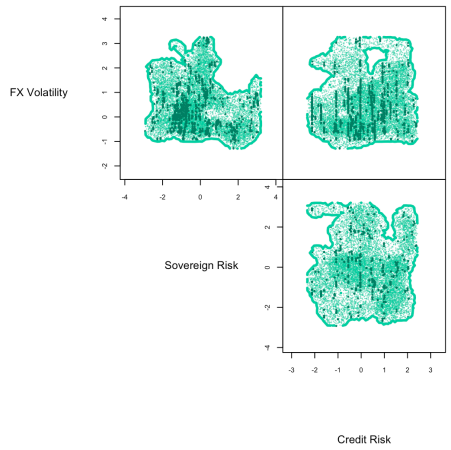
Parameters:

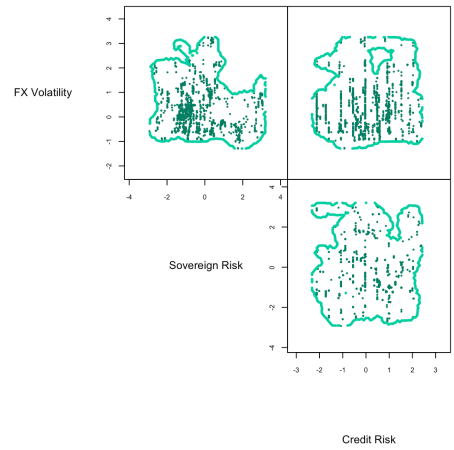
svm.nu: 0.01

svm.gamma: 1

samples.per.point: 100

ν=0.01, γ=1.5





Volume: 33.785289

Random point density: 372.943387

Number of random points: 12600

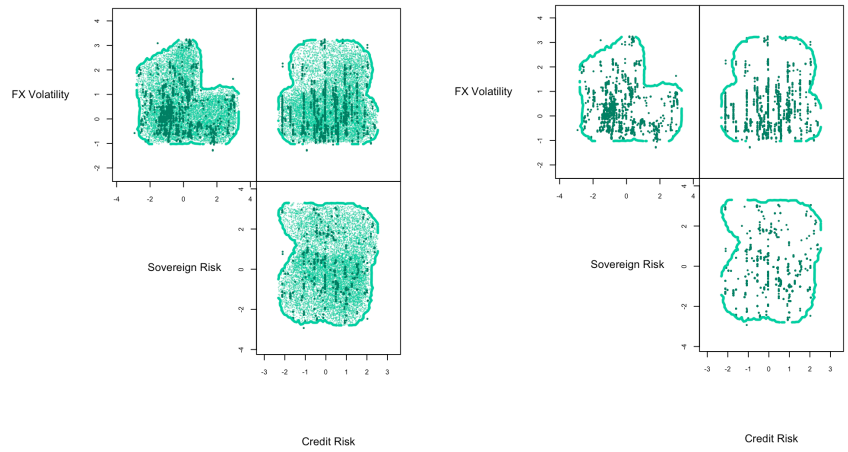
Parameters:

svm.nu: 0.01

svm.gamma: 1.5

samples.per.point: 100

ν=0.05, γ=0.5



Volume: 54.964595

Random point density: 207.406239

Number of random points: 11400

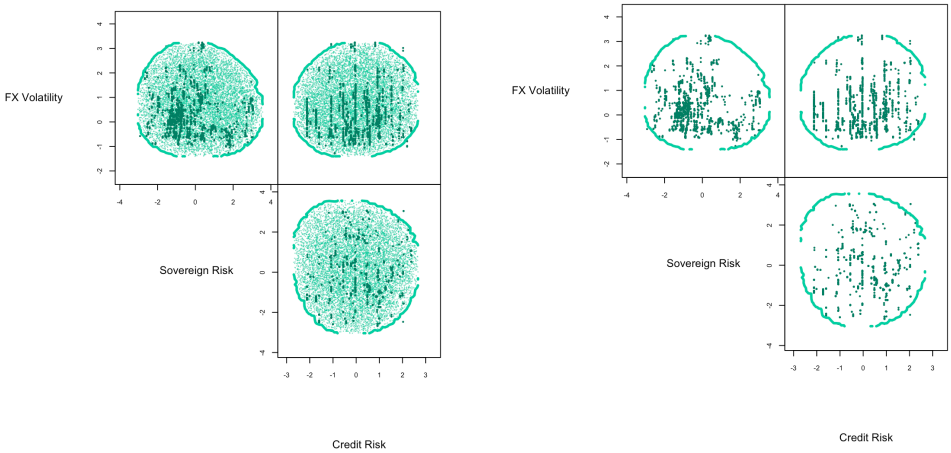
Parameters:

svm.nu: 0.05

svm.gamma: 0.5

samples.per.point: 100

ν=0.05, γ=0.1



Volume: 88.276337

Random point density: 113.280640

Number of random points: 10000

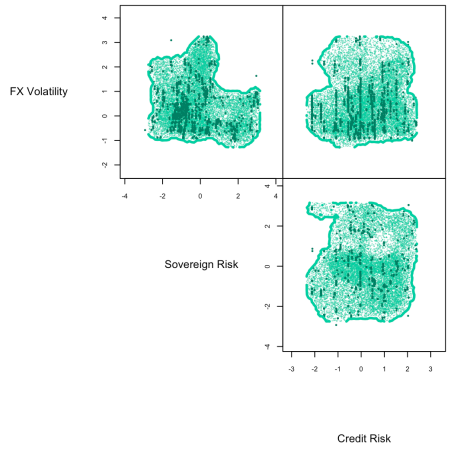
Parameters:

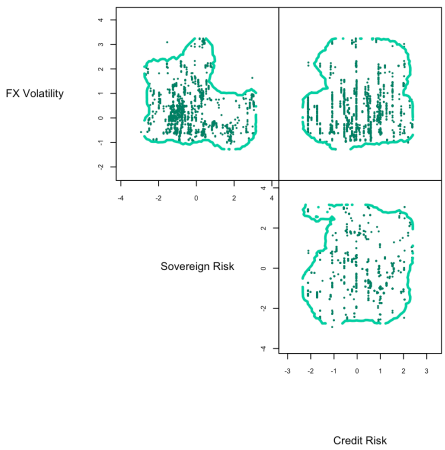
svm.nu: 0.05

svm.gamma: 0.1

samples.per.point: 100

ν=0.05, γ=1





Volume: 40.807836

Random point density: 345.521872

Number of random points: 14100

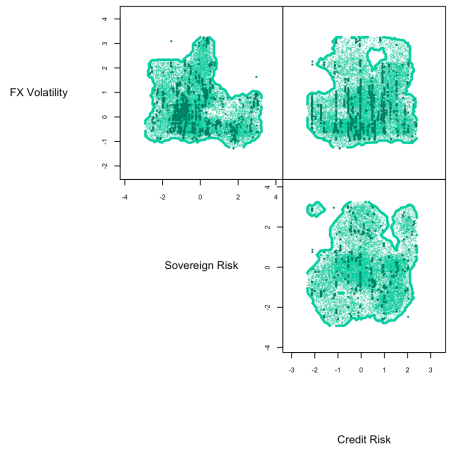
Parameters:

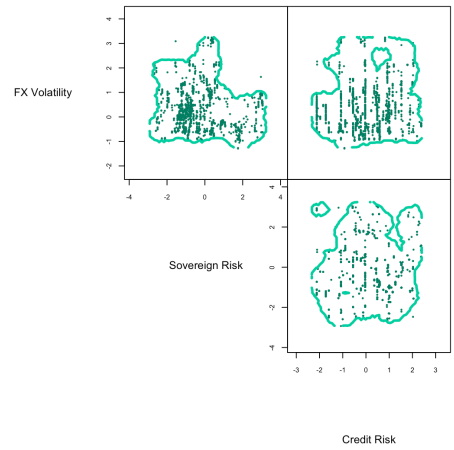
svm.nu: 0.05

svm.gamma: 1

samples.per.point: 100

ν=0.05, γ=1.5





Volume: 30.475568

Random point density: 521.729405

Number of random points: 15900

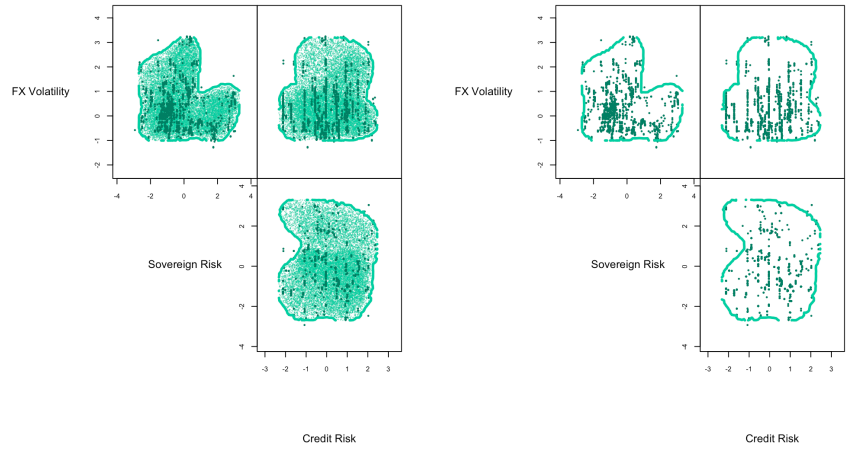
Parameters:

svm.nu: 0.05

svm.gamma: 1.5

samples.per.point: 100

ν=0.1, γ=0.5



Volume: 47.398223

Random point density: 434.615448

Number of random points: 20600

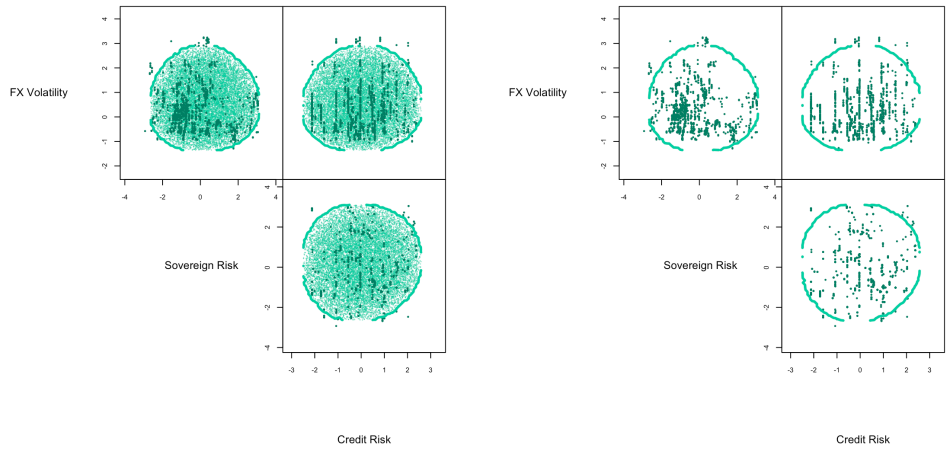
Parameters:

svm.nu: 0.1

svm.gamma: 0.5

samples.per.point: 100

ν=0.1, γ=0.1



Volume: 65.029415

Random point density: 295.251004

Number of random points: 19200

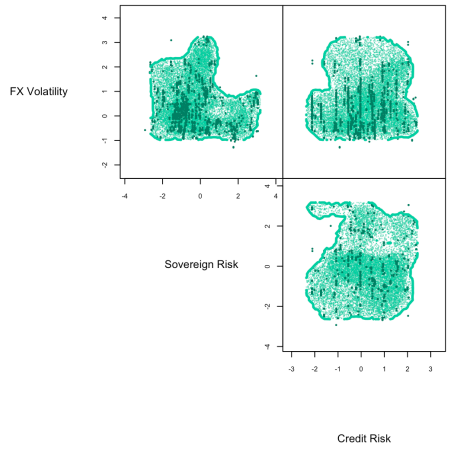
Parameters:

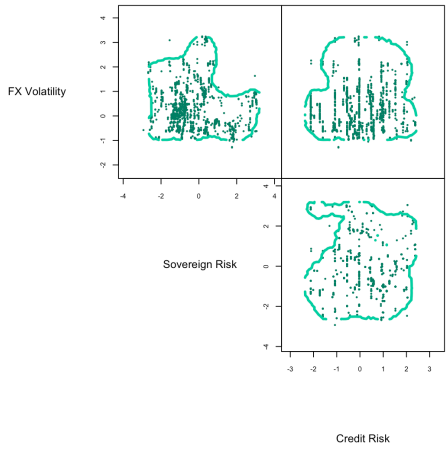
svm.nu: 0.1

svm.gamma: 0.1

samples.per.point: 100

ν=0.1, γ=1





Volume: 35.704715

Random point density: 621.766629

Number of random points: 22200

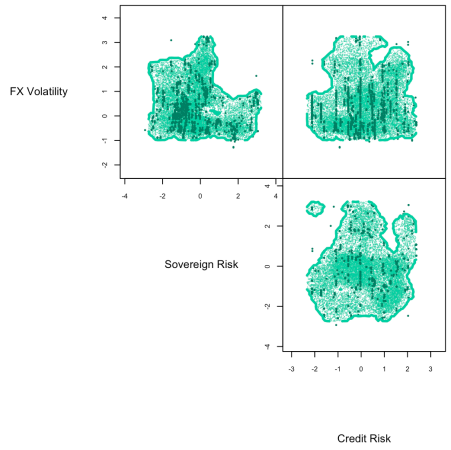
Parameters:

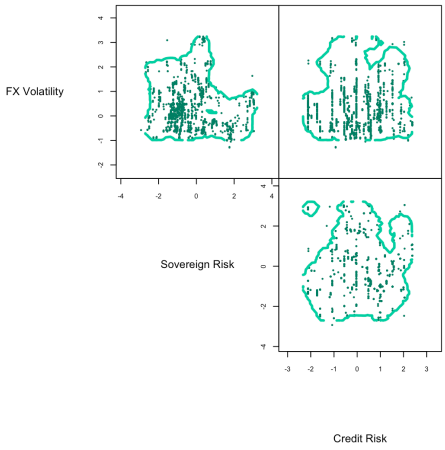
svm.nu: 0.1

svm.gamma: 1

samples.per.point: 100

ν=0.1, γ=1.5





Volume: 27.161032

Random point density: 890.982355

Number of random points: 24200

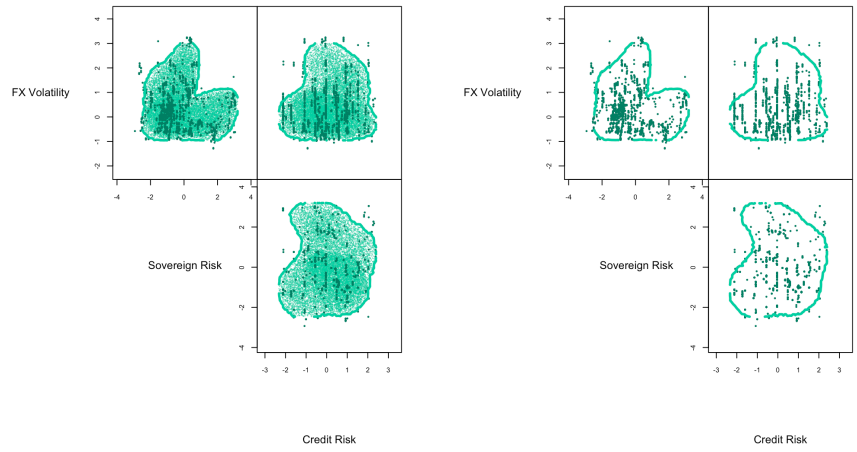
Parameters:

svm.nu: 0.1

svm.gamma: 1.5

samples.per.point: 100

ν=0.2, γ=0.5



Volume: 36.329944

Random point density: 1070.742088

Number of random points: 38900

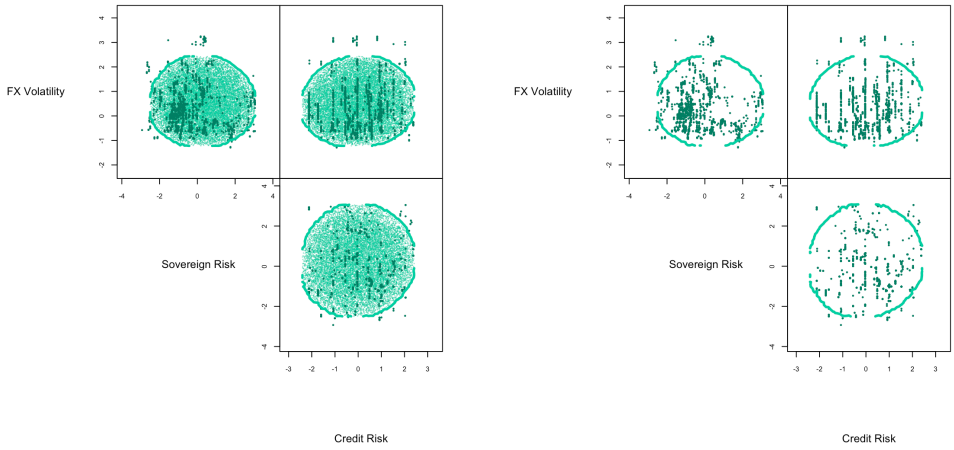
Parameters:

svm.nu: 0.2

svm.gamma: 0.5

samples.per.point: 100

ν=0.2, γ=0.1



Volume: 52.345392

Random point density: 725.947372

Number of random points: 38000

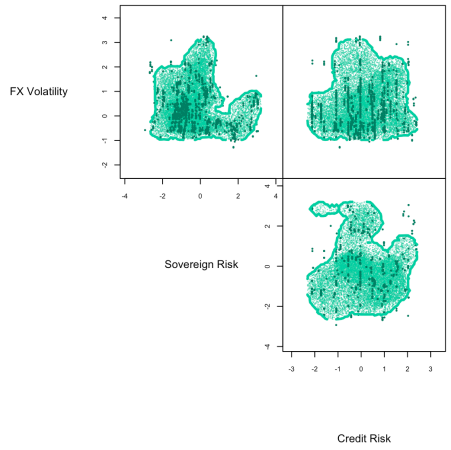
Parameters:

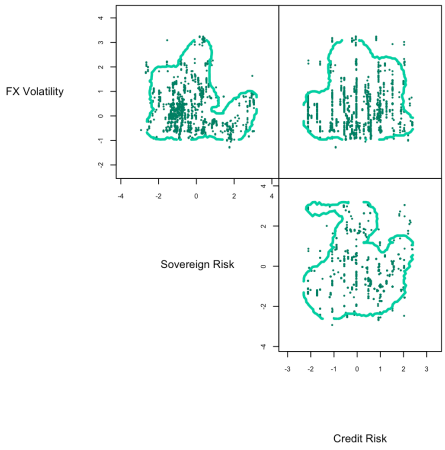
svm.nu: 0.2

svm.gamma: 0.1

samples.per.point: 100

ν=0.2, γ=1





Volume: 27.460900

Random point density: 1456.616507

Number of random points: 40000

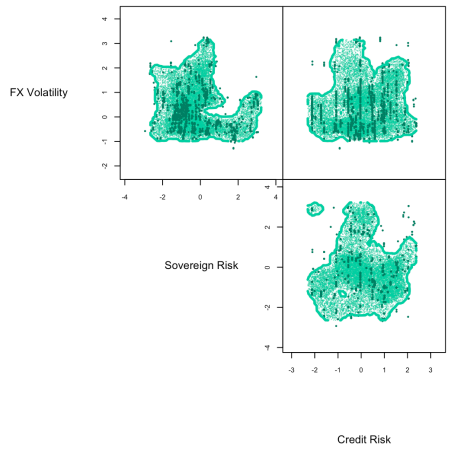
Parameters:

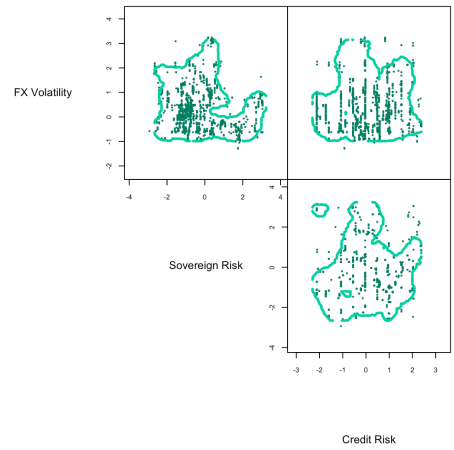
svm.nu: 0.2

svm.gamma: 1

samples.per.point: 100

ν=0.2, γ=1.5





Volume: 20.429936

Random point density: 2036.227651

Number of random points: 41600

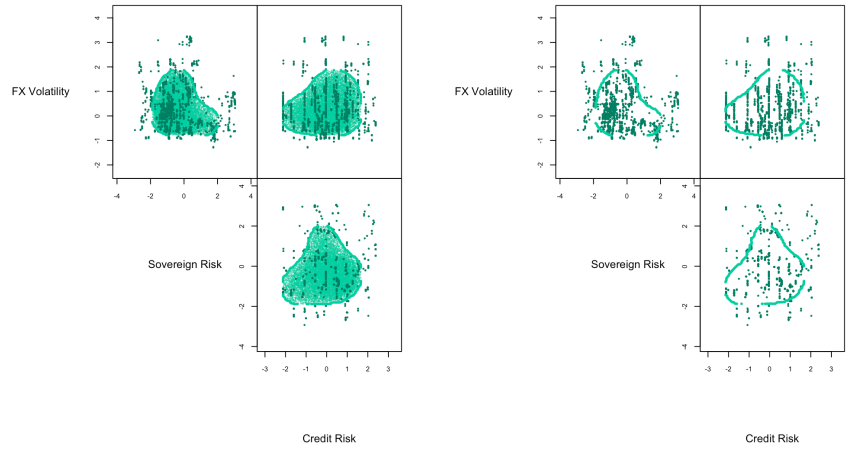
Parameters:

svm.nu: 0.2

svm.gamma: 1.5

samples.per.point: 100

ν=0.5, γ=0.5



Volume: 14.666291

Random point density: 6436.528534

Number of random points: 94400

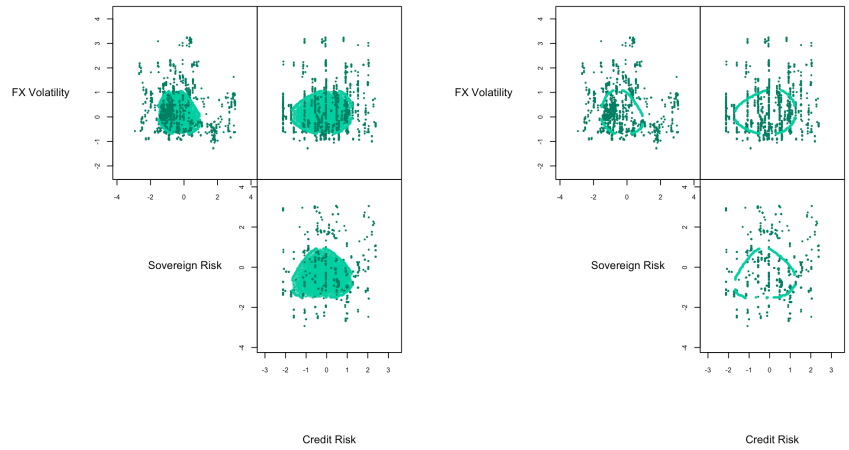
Parameters:

svm.nu: 0.5

svm.gamma: 0.5

samples.per.point: 100

ν=0.75, γ=0.5



Volume: 5.789906

Random point density: 7072.308662

Number of random points: 40948

Parameters:

svm.nu: 0.75

svm.gamma: 0.5

samples.per.point: 29